Instability in composite propellant rockets and improved steady combustion models

Varun Shiva kumar (IITM), H. S. Mukunda (IISc)

DRDL as partners

hsm.cgpl@gmail.com; http://cgpl.iisc.ernet.in

11 February 2016, HEMCI Conference, Hyderabad

What do I want to say?

- Description – *gas phase*; *g*-phase – c-phase coupling
- Back calculating response function from actual p_c – time data
- Traditional expectations, conflicts and issues
- Basis and features of a new heterogeneous quasi 1D (HQ1D) model
- Comparison of predictions of AP-HTPB (data of Miller, Fredrick, Ramakrishna) – ideas for Model for $SrCO_3$, RDX
- Direction of results, Additional calibration data required, Summary of progress.

G-phase oscillatory combustion behavior - Ruben's tube

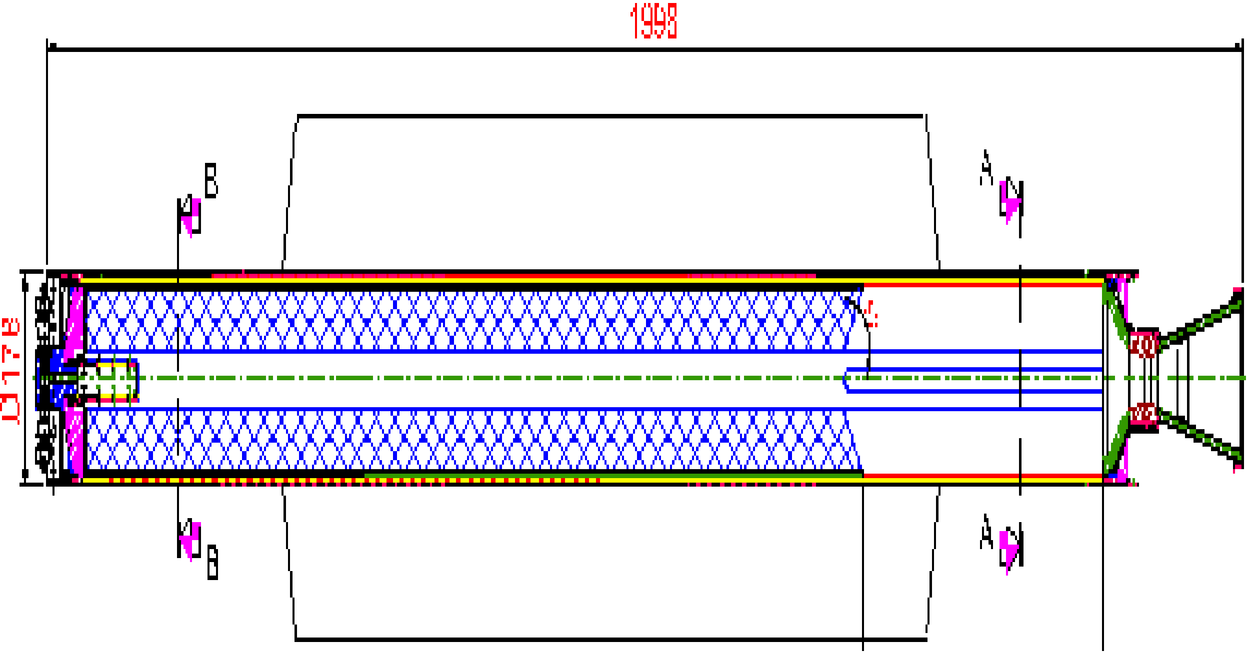

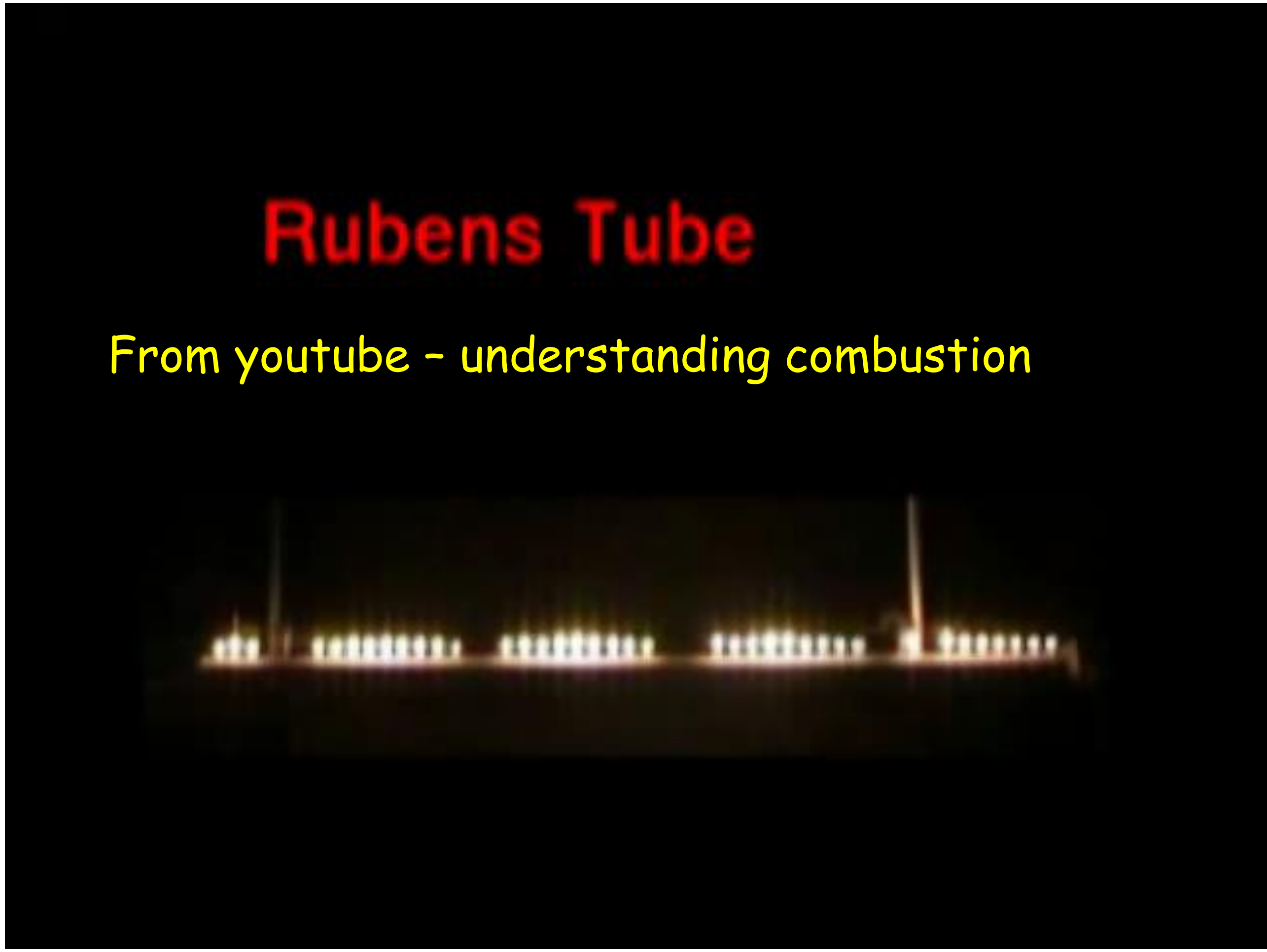

Rough turbulent combustion vs. Combustion instability

- Rough combustion should be distinguished from classical turbulent combustion that looks rough and noisy. Turbulent combustion spectra (kinetic energy of fluctuations vs. wave number) have classical decay behavior.
- Rough combustion <u>of concern in operating systems</u> is called “combustion instability”.

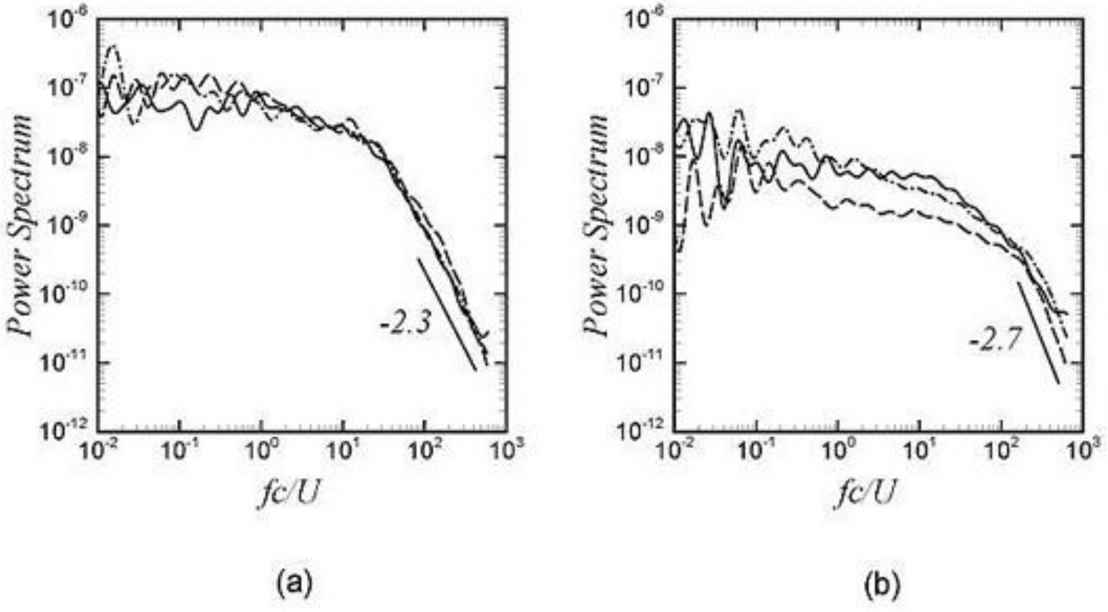

Normal and acceptable

Power
p’ or v’²

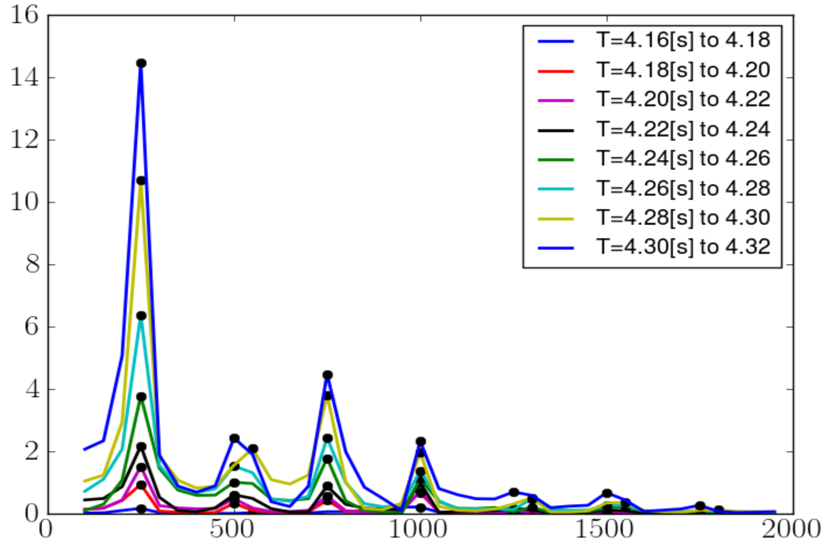

Disastrous and unacceptable

f, Hz *f τ* or *fα/ŕ²*

Steady combustion vs. Unsteady combustion

Smooth p_c-time profile

Fluctuations < 0.5 %

p_c vs. time with undesirable irregular fluctuations (> 2 %)

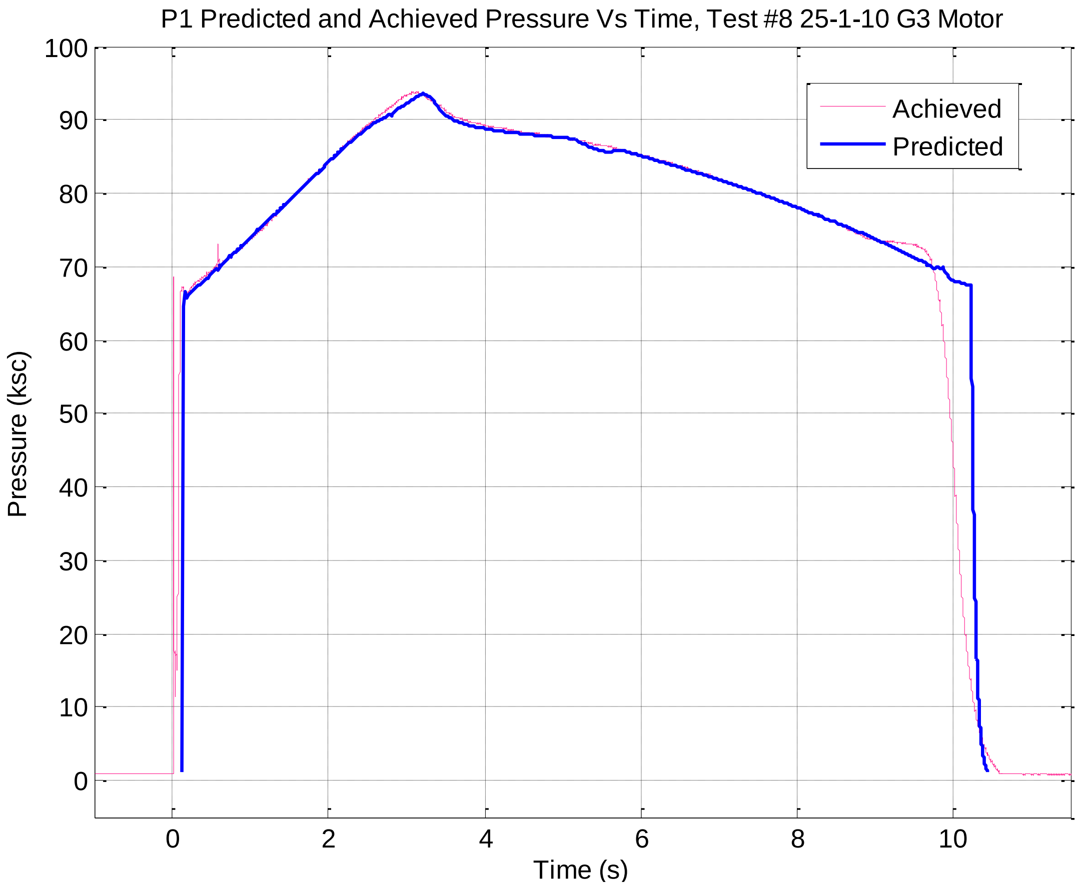

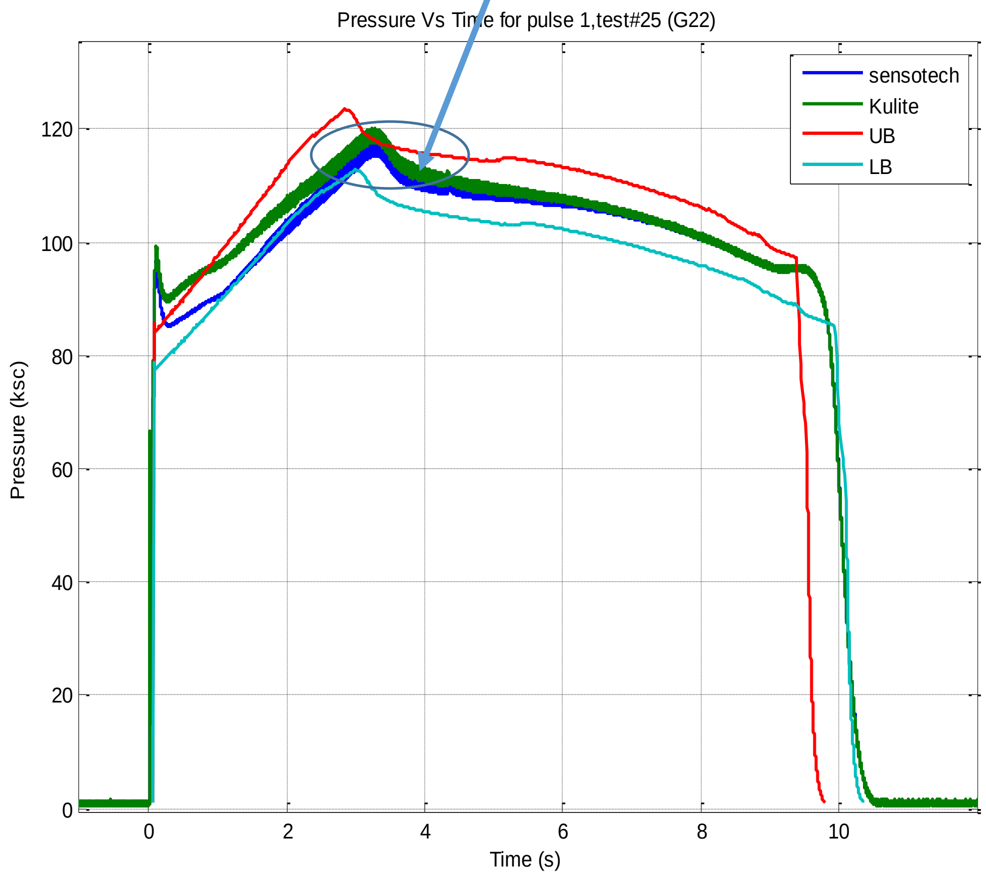

Example here is of solid rockets. But the features are true for all systems – After burners, main combustor as well

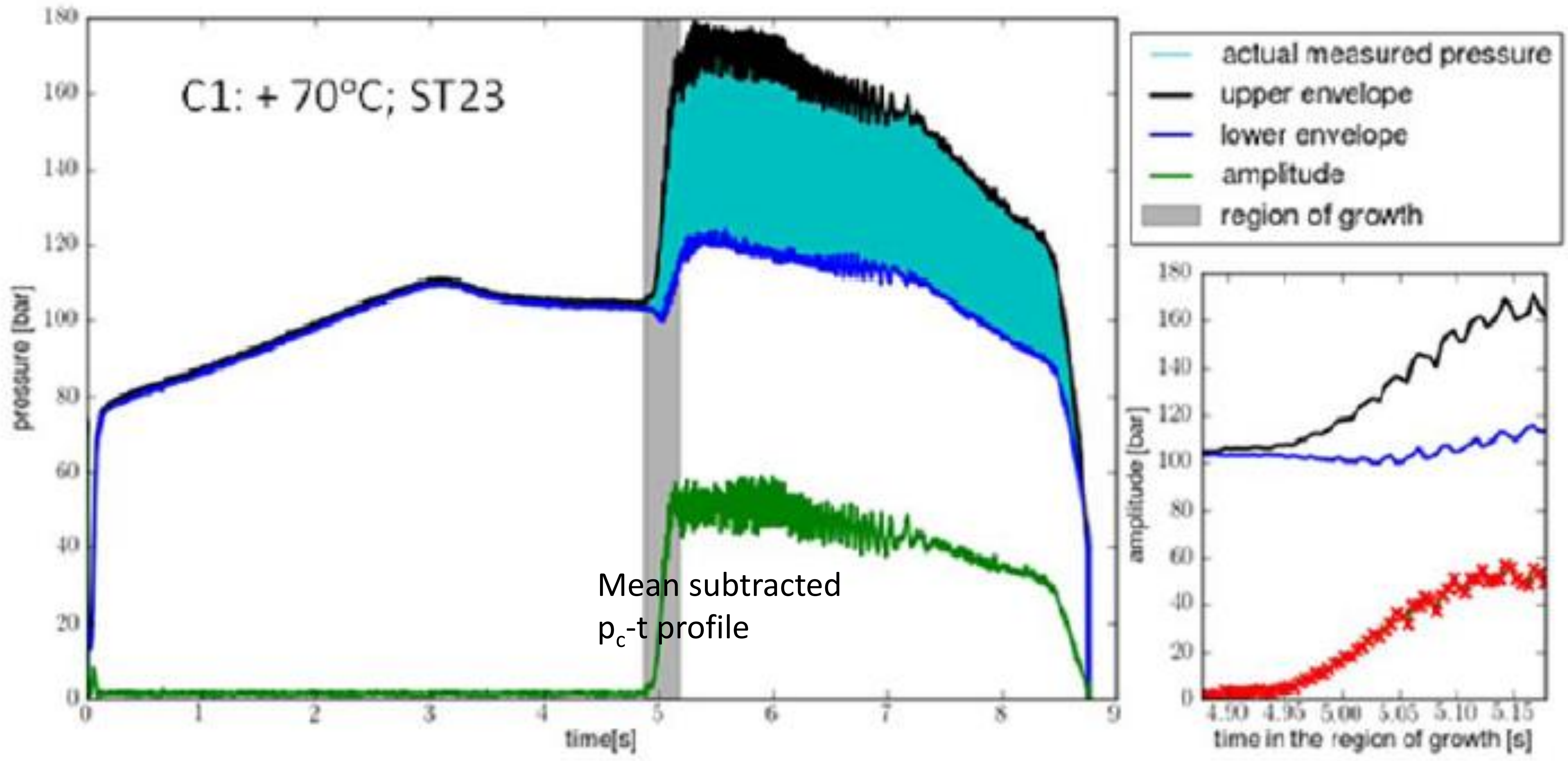

Chamber pressure-time curve of a tactical rocket. Till 4.85 s, the combustion process is smooth. At this time, there are fluctuations that build up in 200 ms with visible oscillation amplitude of 15 bar (atm) and a shift of mean pressure (called DC shift) itself by 50 atm with an expected mean pressure of 120 atm.

How to get α_{Motor} from actual motor tests?

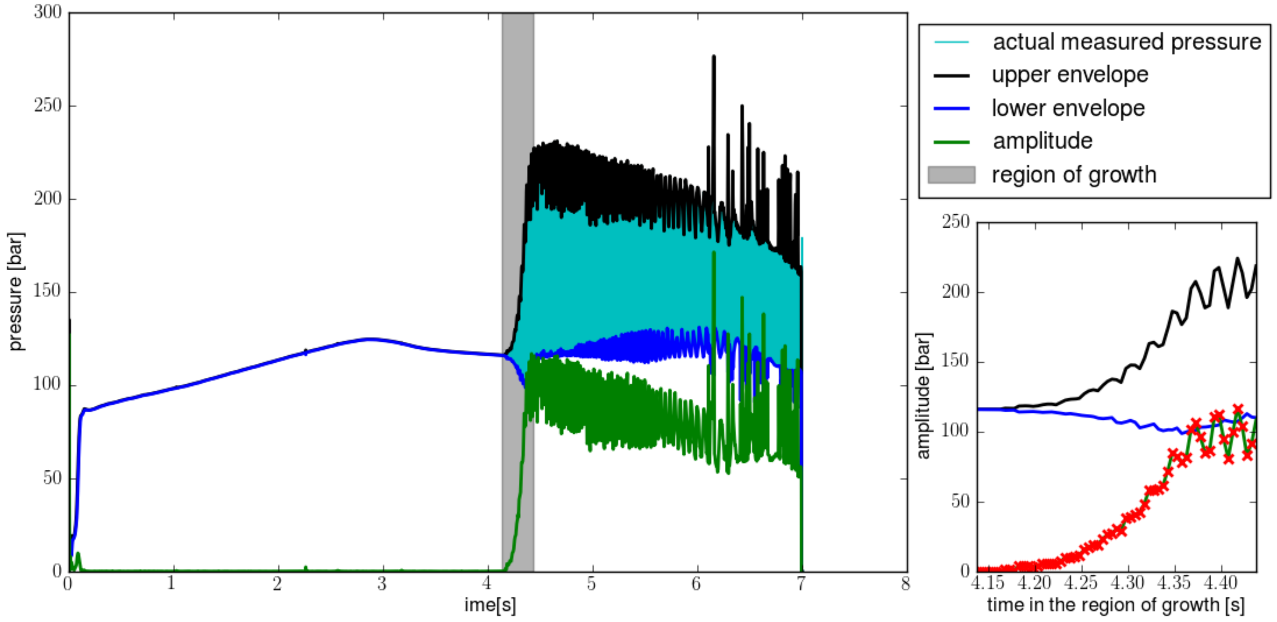

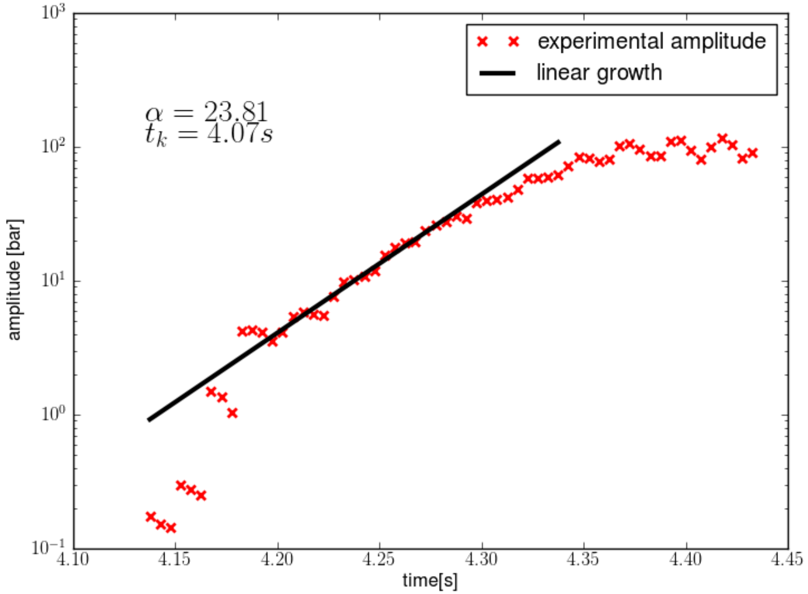

- Near the onset of instability the growth ratio is plotted (semi-log) with respect to time.
- The amplitude grows to near exponent through most of the growth
- The exponent is obtained as α_{motor}

C1: + 70°C; ST23 Water –fall plot

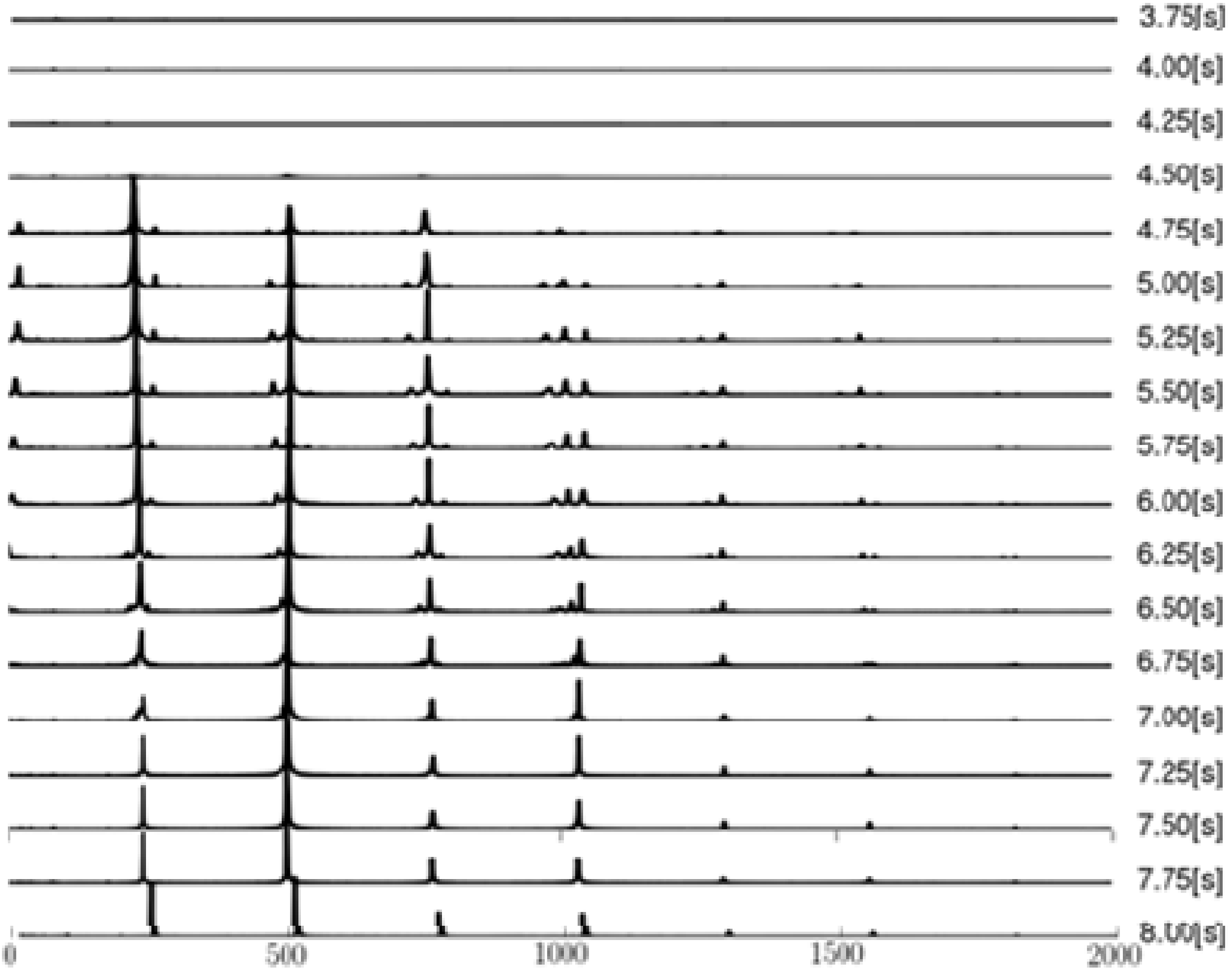

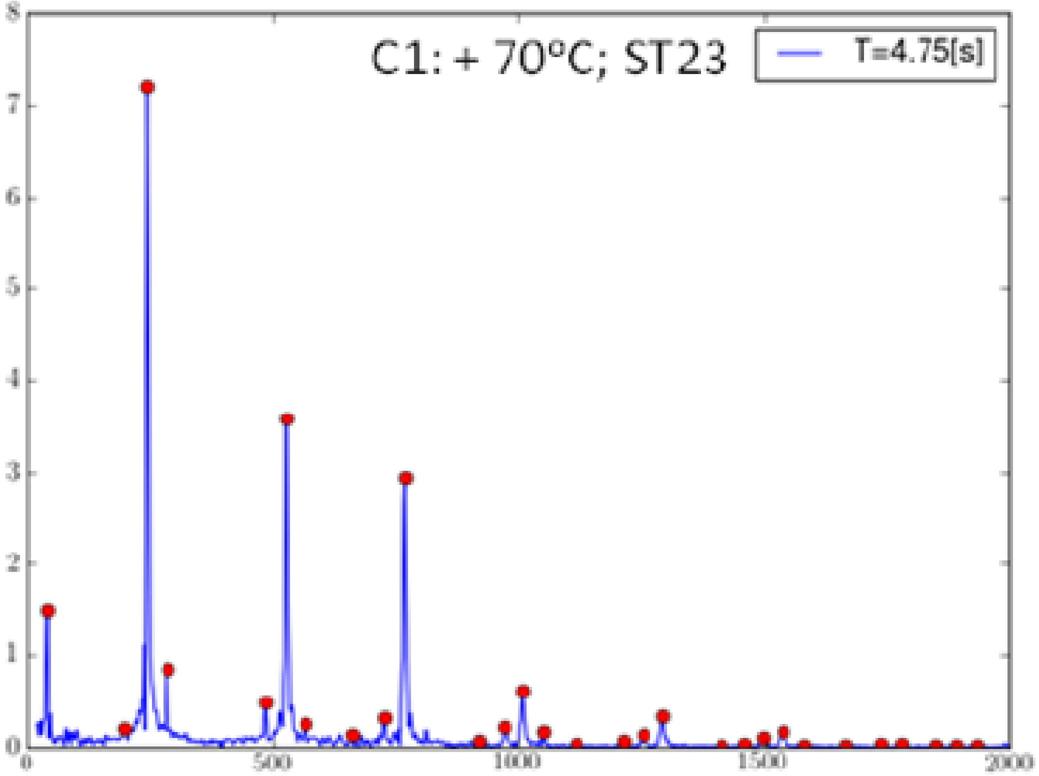

We can do a spectral analysis of the time-sliced pressure time curve and see how the instability is developing. This is set out in the water-fall plot. The specific frequencies – about 250, 500, 750 and 1000 Hz are the ones excited here.

time = 4.17s

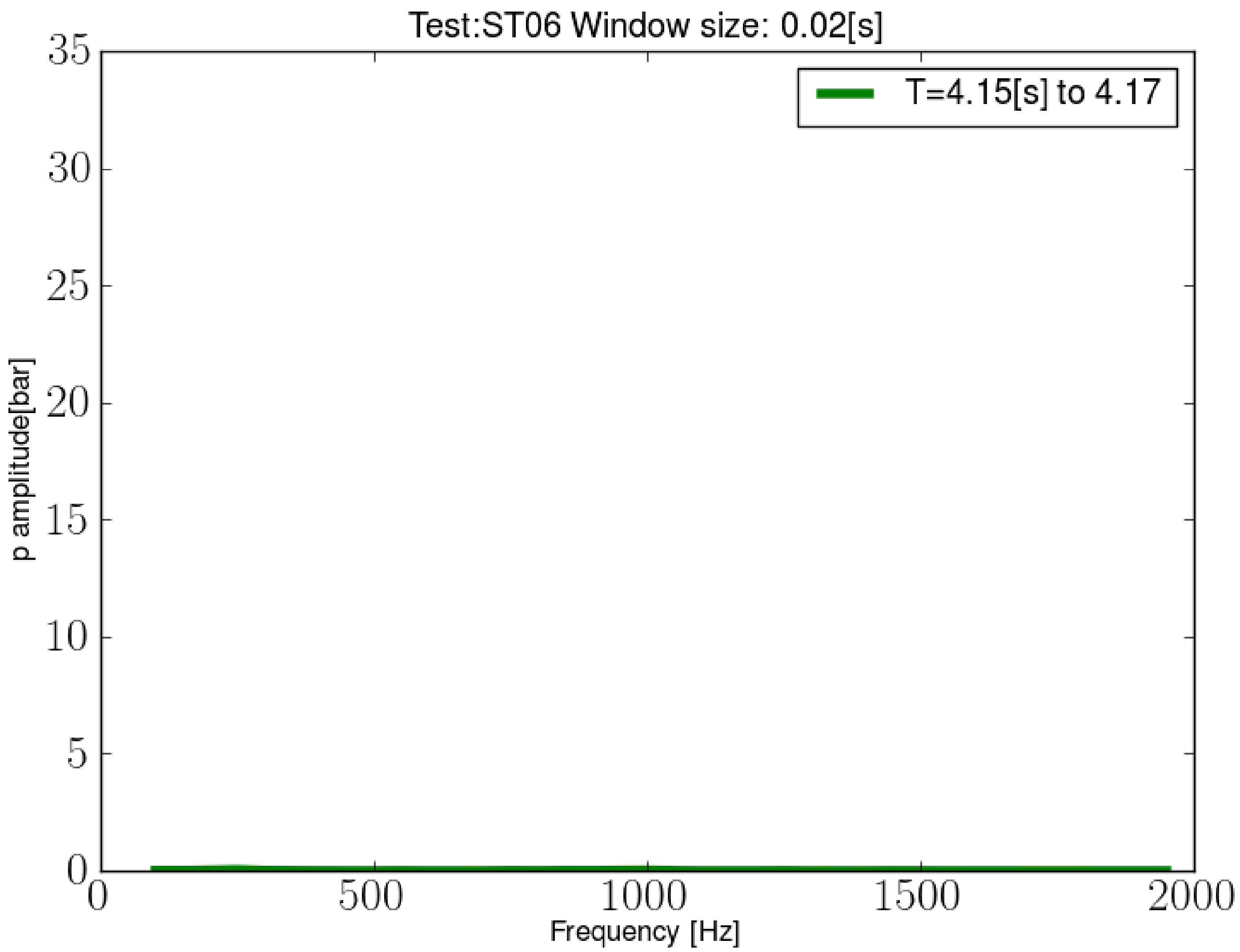
Test:ST06 Window size: 0.02[s]
T=4.15[s] to 4.17
p amplitude[bar]
Frequency [Hz]
0
5
10
15
20
25
30
35
0
500
1000
1500
2000

Time = +20 ms

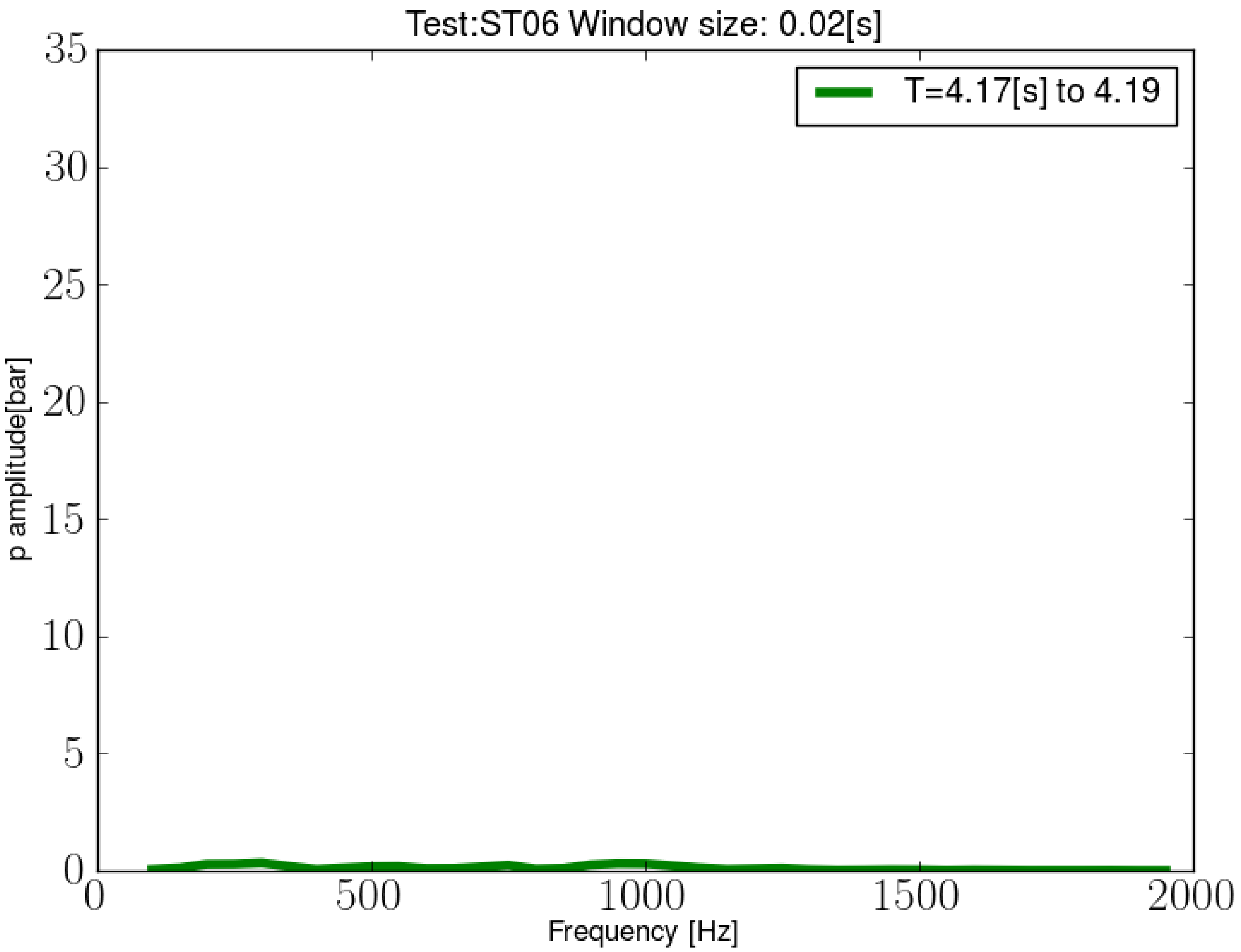

Test:ST06 Window size: 0.02[s]
T=4.17[s] to 4.19
p amplitude[bar]
Frequency [Hz]
35
30
25
20
15
10
5
0
0
500
1000
1500
2000

Time = +40ms

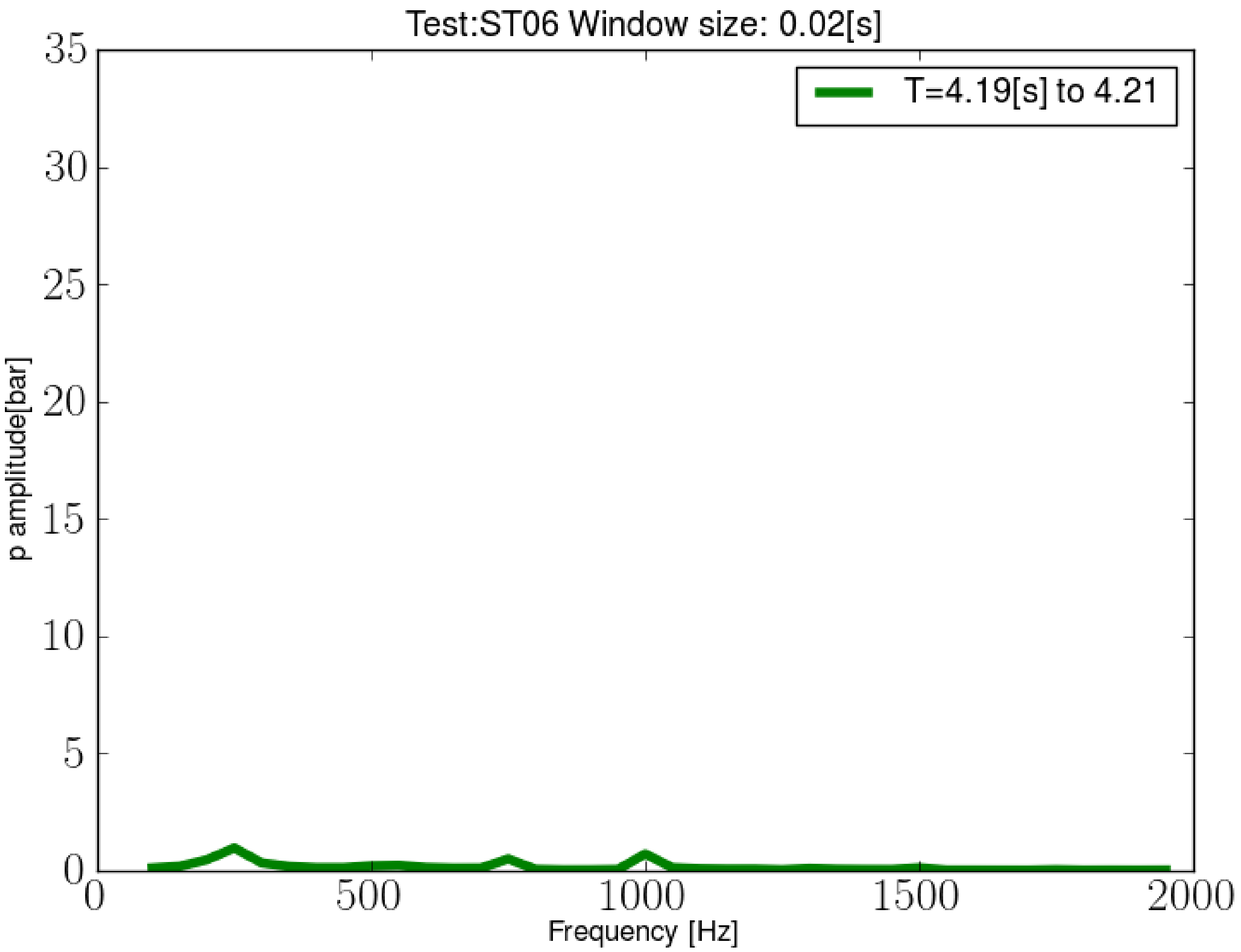

Test:ST06 Window size: 0.02[s]
T=4.19[s] to 4.21
p amplitude[bar]
35
30
25
20
15
10
5
0
0
500
1000
1500
2000
Frequency [Hz]

Time = +60ms

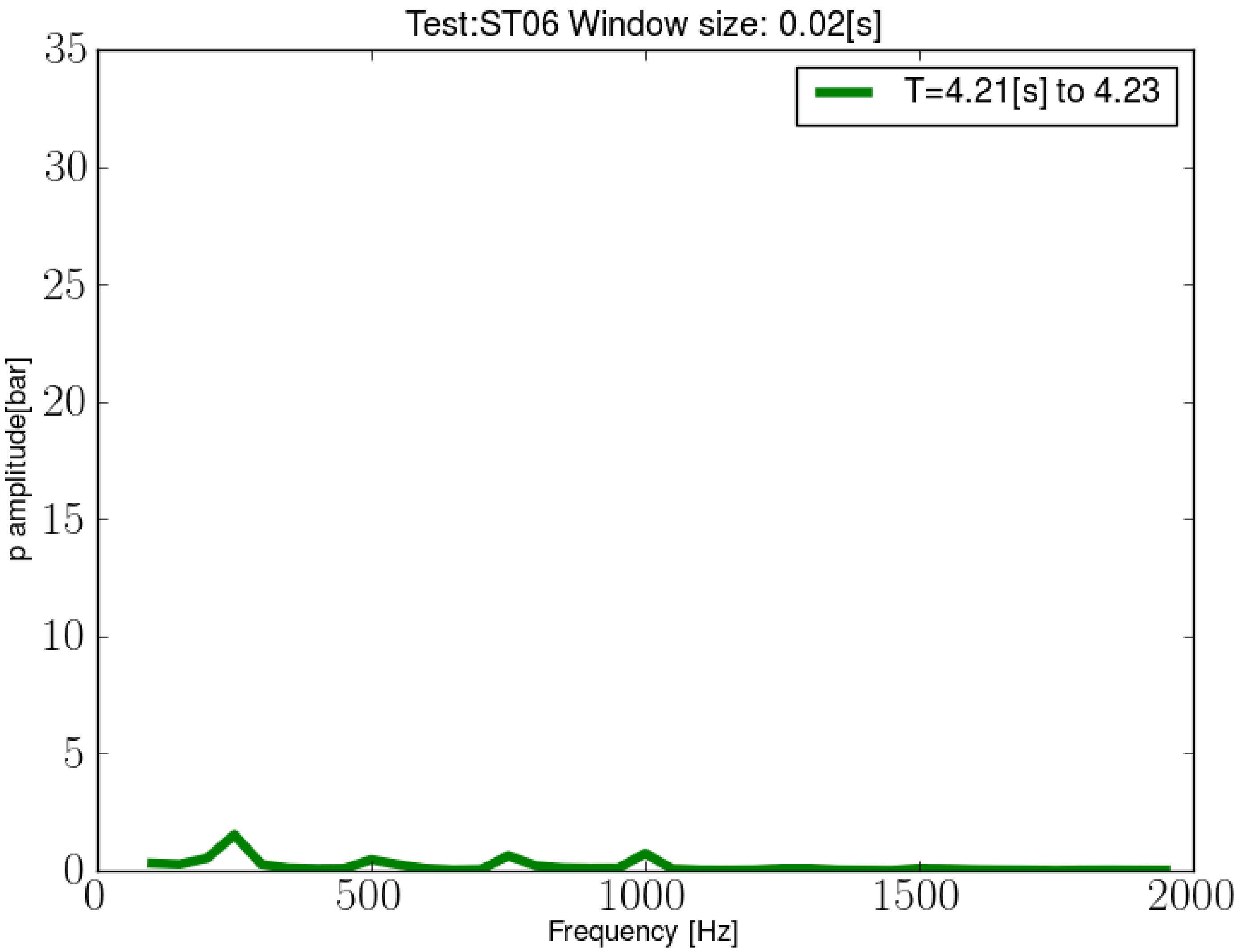

Test:ST06 Window size: 0.02[s]
T=4.21[s] to 4.23
p amplitude[bar]
35
30
25
20
15
10
5
0
0
500
1000
1500
2000
Frequency [Hz]

Time = +80ms

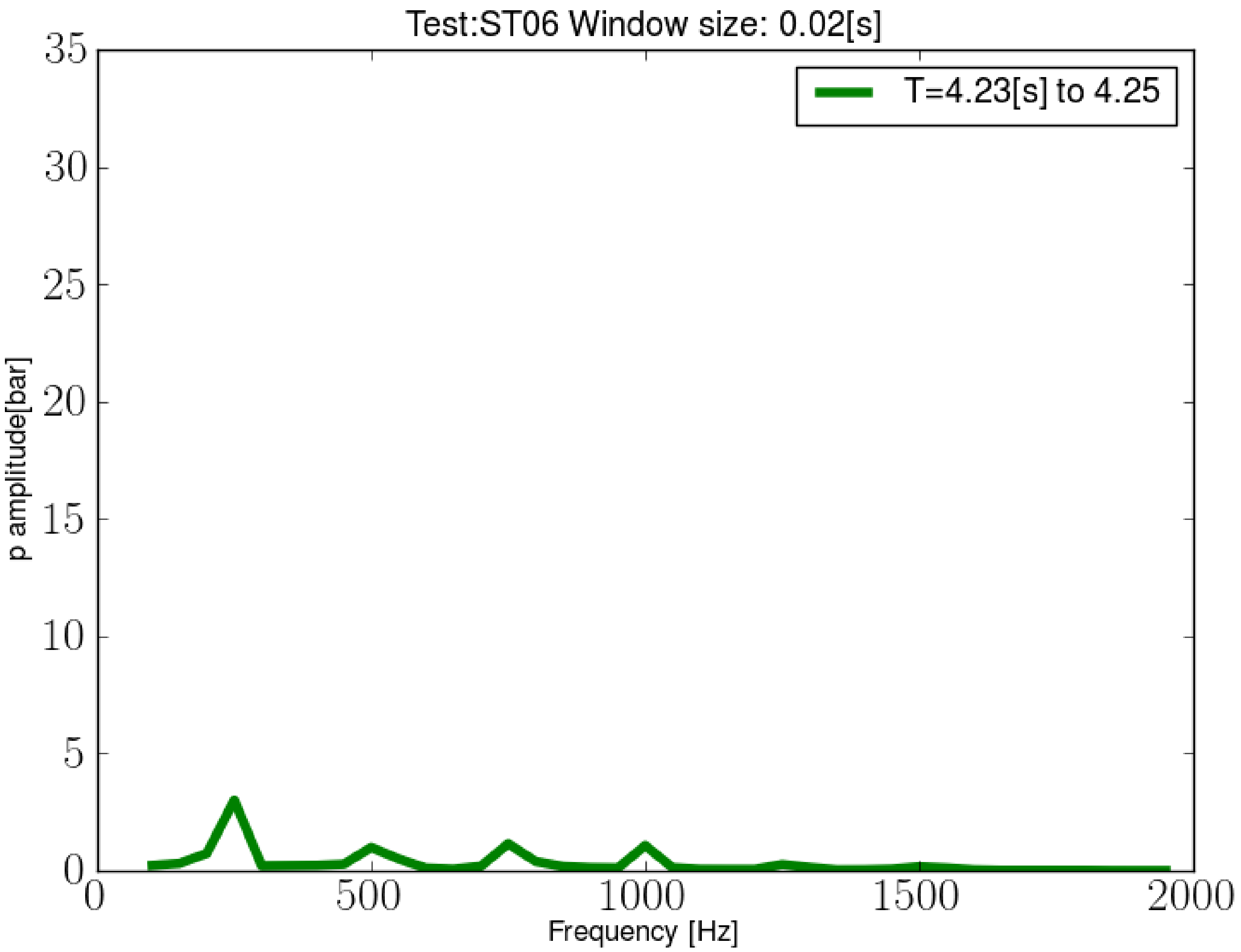

Test:ST06 Window size: 0.02[s]
T=4.23[s] to 4.25
p amplitude[bar]
Frequency [Hz]
0
5
10
15
20
25
30
35
0
500
1000
1500
2000

Time = +80ms

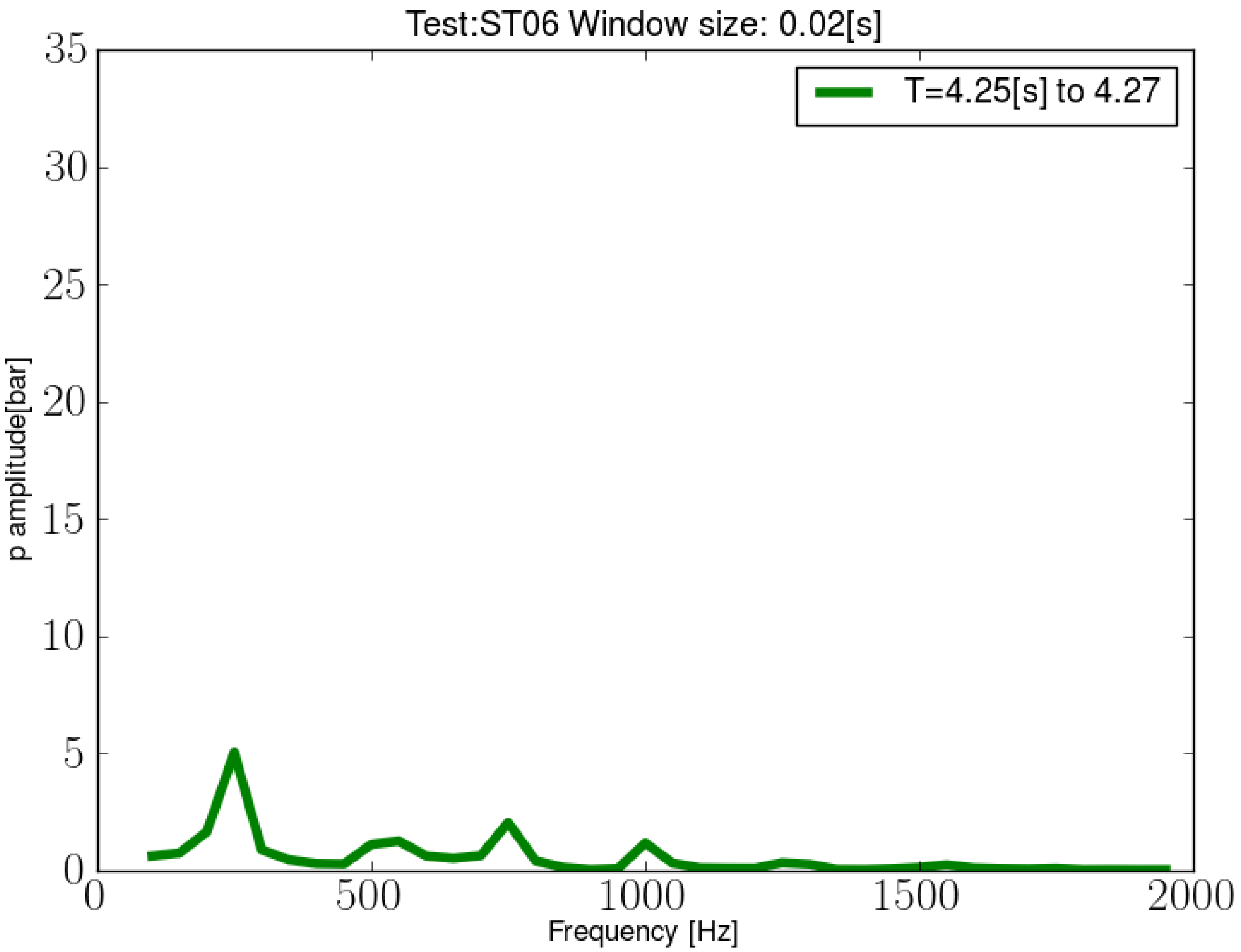

Test:ST06 Window size: 0.02[s]
T=4.25[s] to 4.27
p amplitude[bar]
Frequency [Hz]
0
5
10
15
20
25
30
35
0
500
1000
1500
2000

Time = +100ms

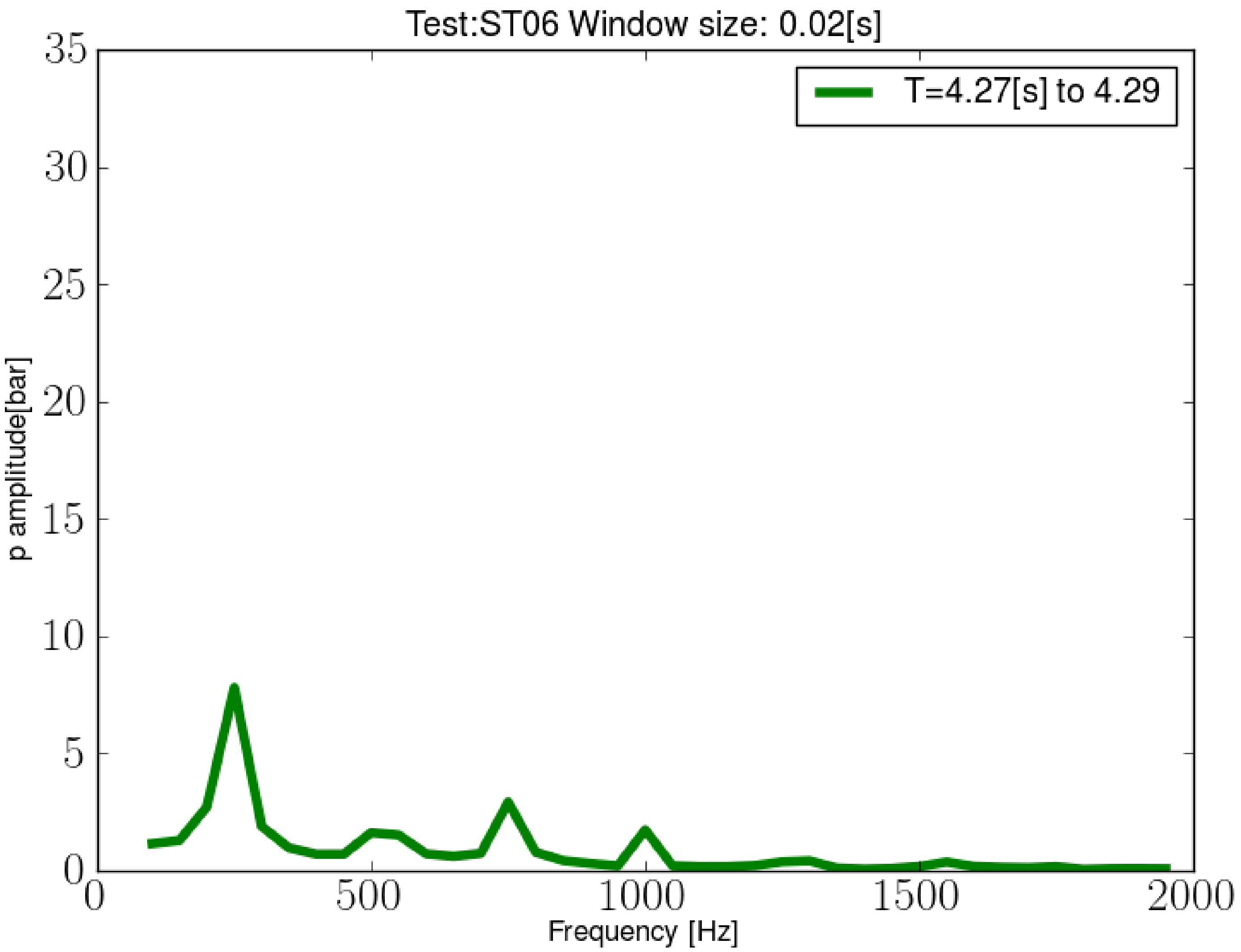

Test:ST06 Window size: 0.02[s]
T=4.27[s] to 4.29
p amplitude[bar]
0
5
10
15
20
25
30
35
0
500
1000
1500
2000
Frequency [Hz]

Time = +120ms

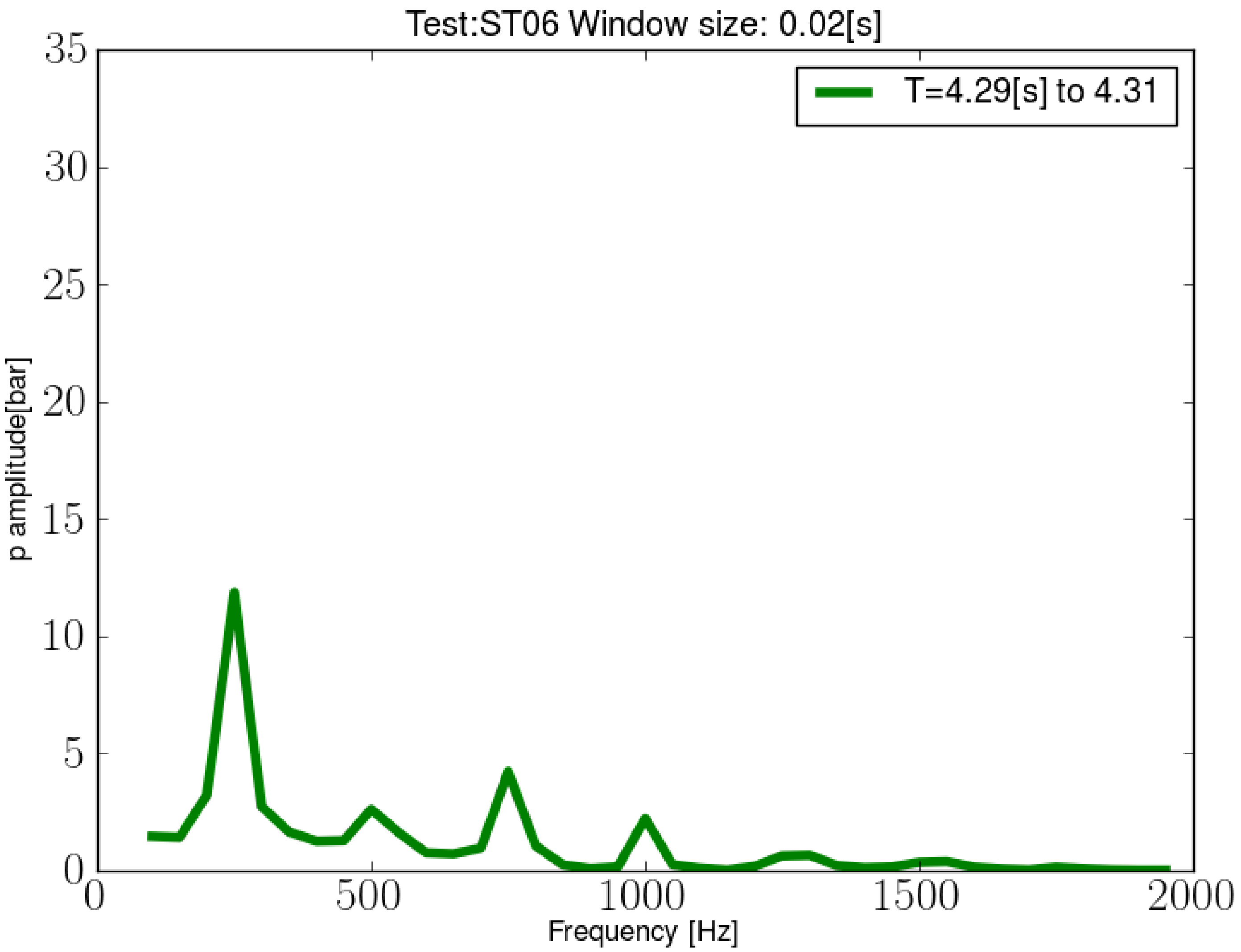
Test:ST06 Window size: 0.02[s]
T=4.29[s] to 4.31
p amplitude[bar]
Frequency [Hz]
0
5
10
15
20
25
30
35
0
500
1000
1500
2000

Time = +140ms

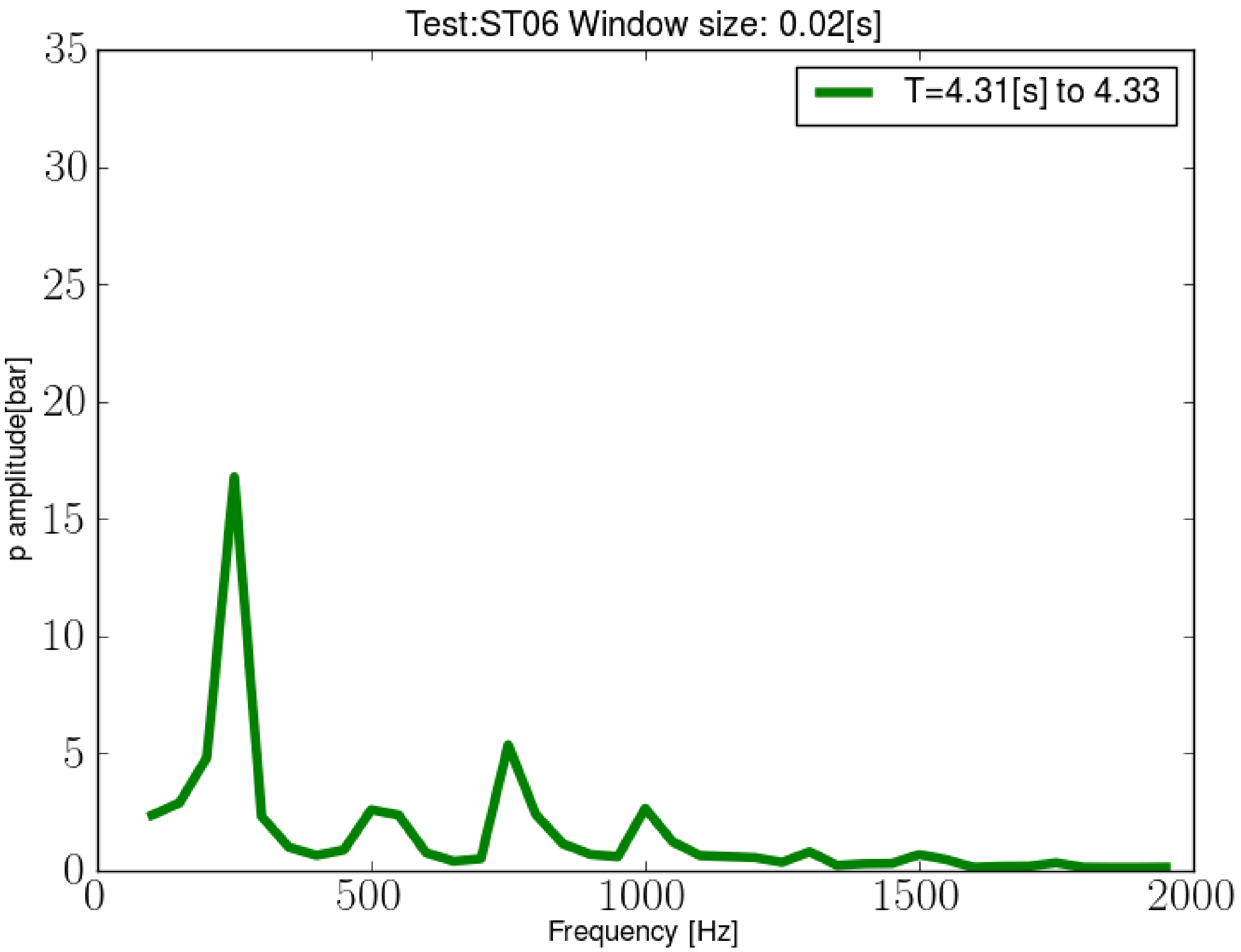

Test:ST06 Window size: 0.02[s]
T=4.31[s] to 4.33
p amplitude[bar]
Frequency [Hz]
0
5
10
15
20
25
30
35
0
500
1000
1500
2000

Time = +160ms

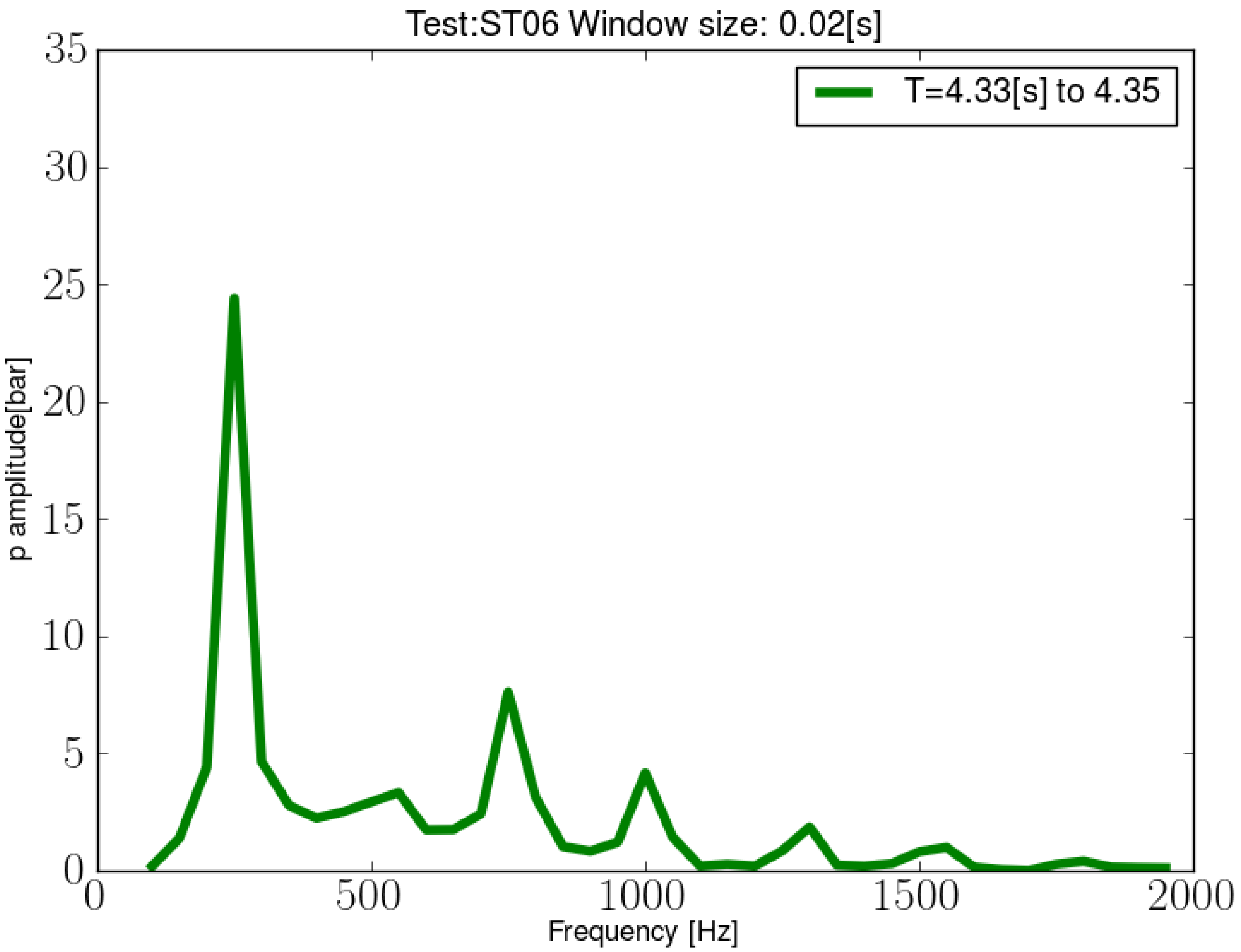

Test:ST06 Window size: 0.02[s]
T=4.33[s] to 4.35
p amplitude[bar]
Frequency [Hz]
0
5
10
15
20
25
30
35
0
500
1000
1500
2000

Time = +180ms

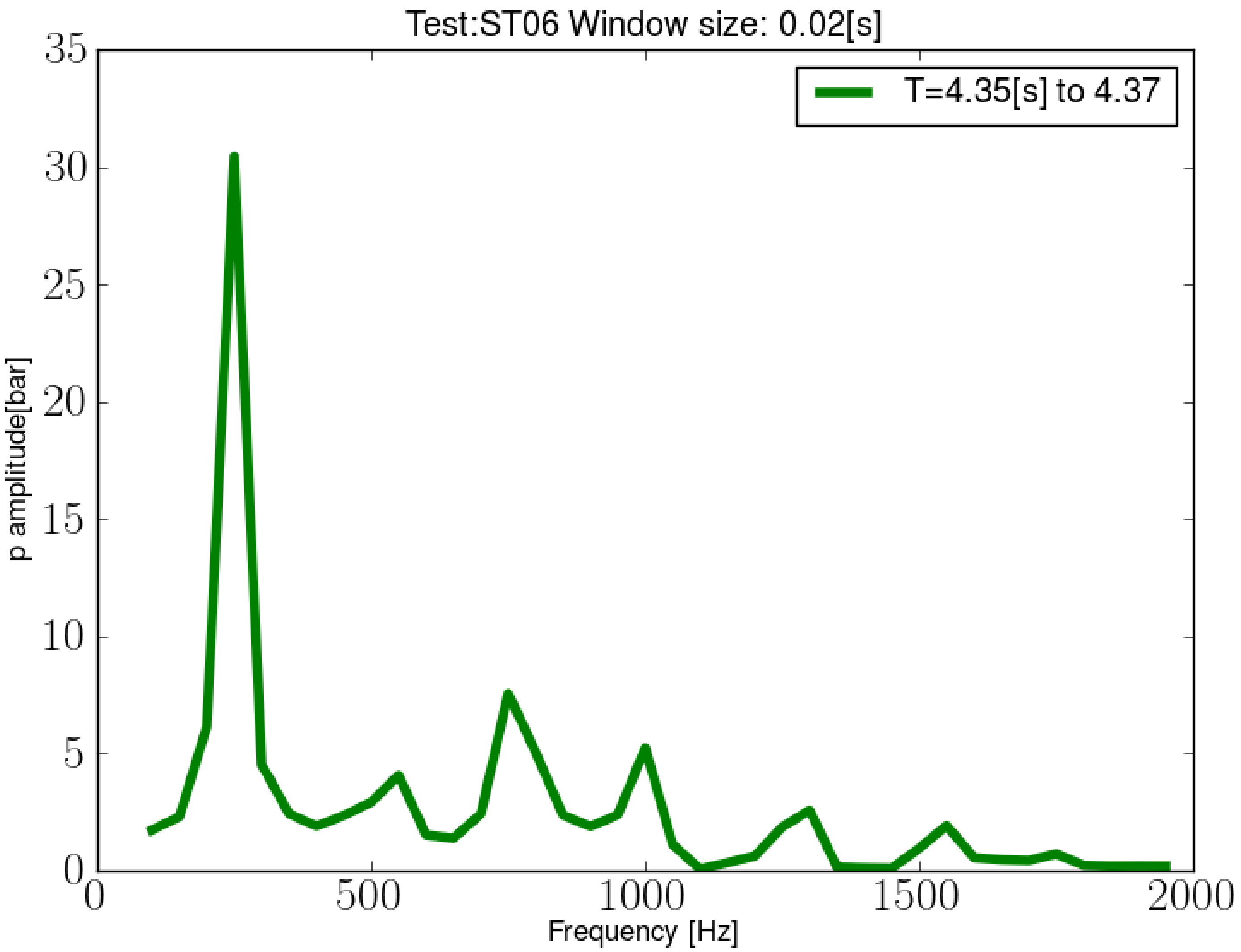

Test:ST06 Window size: 0.02[s]
T=4.35[s] to 4.37
p amplitude[bar]
Frequency [Hz]
0
5
10
15
20
25
30
35
500
1000
1500
2000

Time = +200ms

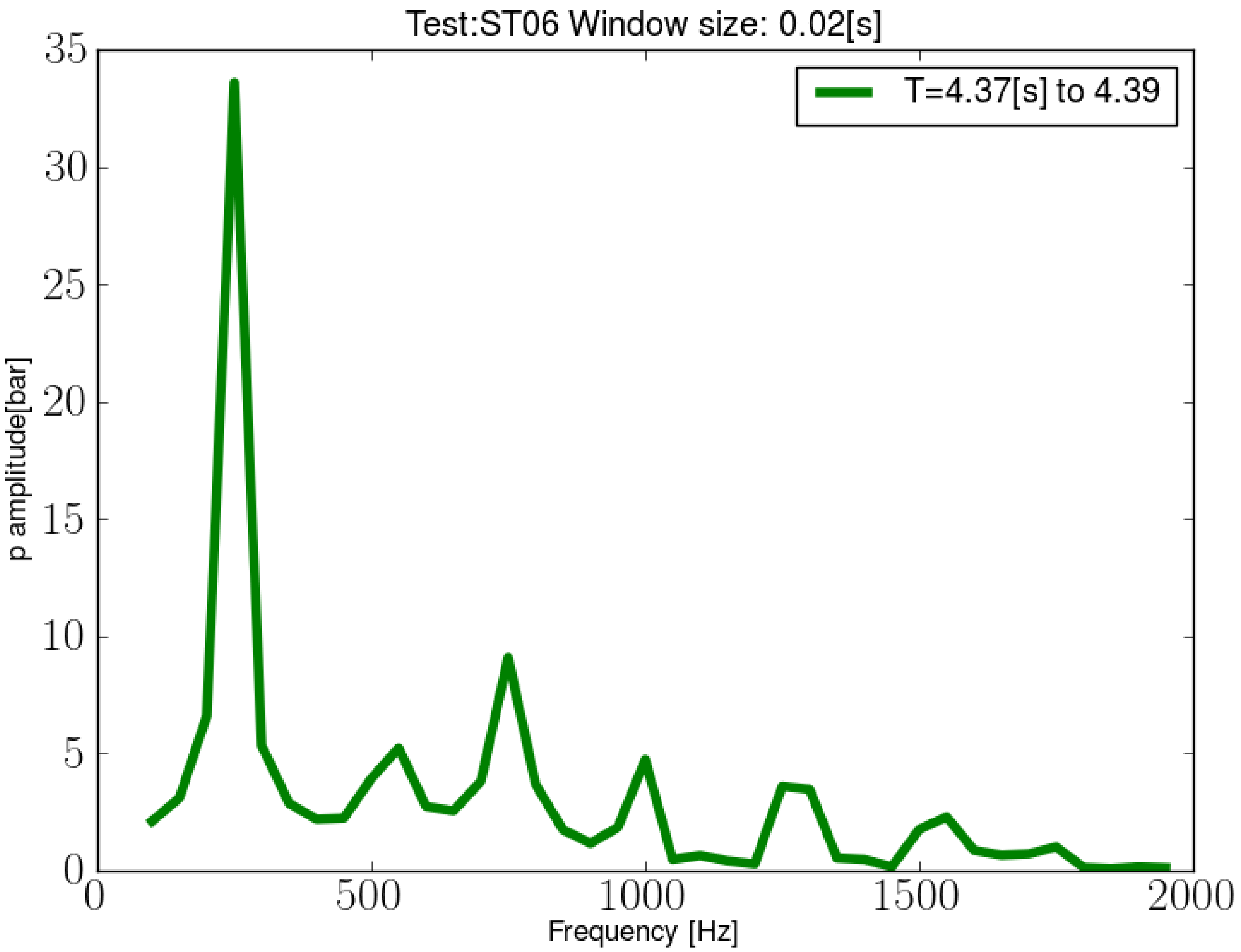

Test:ST06 Window size: 0.02[s]
T=4.37[s] to 4.39
p amplitude[bar]
Frequency [Hz]
0
5
10
15
20
25
30
35
0
500
1000
1500
2000

Approximate flow turning and nozzle losses

Injection velocity ~ 1m/s

Flow turning losses

$$\alpha_{FT} = \frac{V_{\text{inj}}}{R_p}$$

Port Radius

Nozzle losses

$$\alpha_N = 2\frac{V_{\text{inj}}}{R_p}$$

These have been established by Varun and the DRDL CFD team accurately ; DRDL team has calculated them by several means

Getting motor growth rate and Response function

$p'/p_{mean} \sim exp\ (\alpha_{Motor}\ t)$

The growth rate due to the propellant, α_{prop} is related to α_p by

$$\alpha_{Motor} = \alpha_P - \alpha_{FT} - \alpha_N$$

$$\frac{dp_c}{dt} = \frac{RT_c}{V}(\rho_p A_b \dot{r} - p_c A_t / c^*)$$

$p_c = p_{mean} + p'$, *etc leads to*

The propellant response function is therefore,

$\boldsymbol{R_p} = 1 + [A_p/A_t][\ \alpha_p\ (mode\ no./f_{mode})]\ [\sqrt{\gamma}\ /\{2\Gamma(\gamma)\}]$

It is important to obtain R_p vs. dimensionless frequency $f_s = f\alpha_{D1}/\acute{r}_s^2$

Table 11: Thermal diffusivity of the grouped ingredients

Temp, °C	Thermal diffusivity, α_D, mm^2/s					
	AP1	AP2	RDX	Al	Polymers	Inorganics
-30	0.270	0.15	0.160	49.6	0.110	0.050
+25	0.250	0.11	0.145	49.6	0.107	0.040
+70	0.230	0.09	0.130	49.6	0.105	0.030

Note: The thermal diffusivity of AP from different sources (literature as well as in actuality because of the presence of ionic elements like K)

The thermal diffusivity is a fairly strong function of the initial temperature; higher the temperature, lower is the thermal diffusivity

Therefore, Propellant and some ingredients must be characterized for size distribution (AP) and thermo-physical properties.

The results

$$R_p = \frac{nB + \cancel{n_s(\lambda - 1)}}{\lambda + \frac{A}{\lambda} - (1 + A) + B}$$

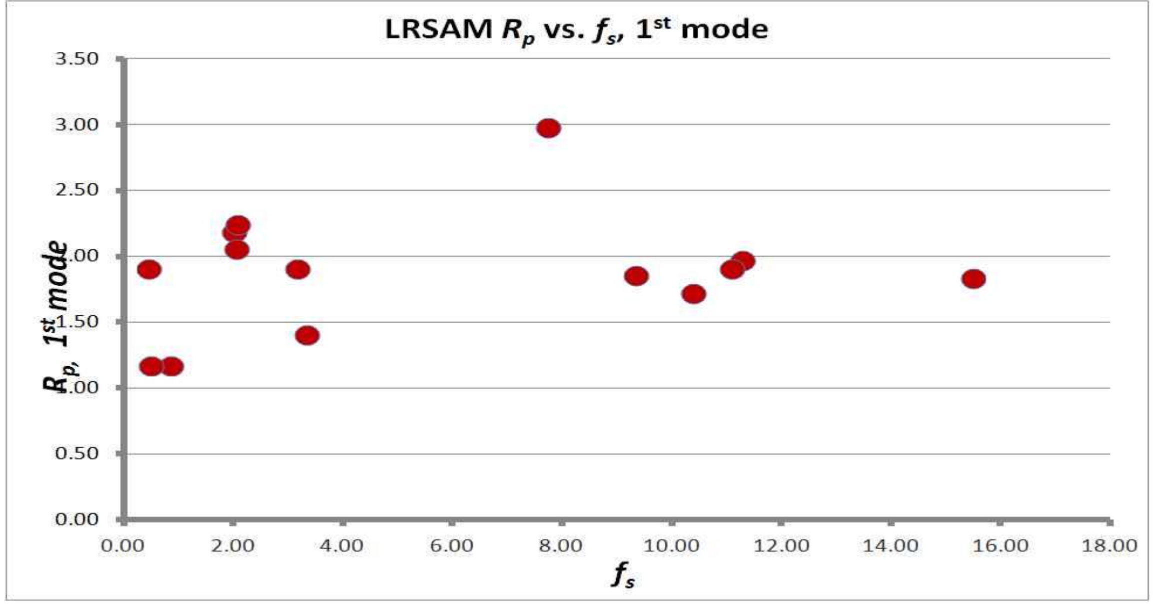

Prop	Test	T_{ini} °C	R_p	f_{s2}
C1	ST06	+58	3.19	2.16
	ST07	+58	2.65	2.03
	ST23	+70	3.52	2.06
C2	ST17	-30	2.53	3.15
C3	ST15	+70	2.04	3.33
C4	ST20	-30	2.87	11.31
	ST21	+20	2.97	9.32
	ST22	+71	1.85	7.25
C6	ST24	-30	3.31	11.11
C7	ST25	+70	2.16	7.06
	ST26	-30	4.21	8.79
	ST27	-30	3.48	7.72
C8	ST30	+70	3.76	15.47
C1b	ST32	+25	3.21	10.37
C9	ST38	+70	1.95	0.49
	ST39	-30	1.22	0.91
	ST49	+70	1.85	0.50

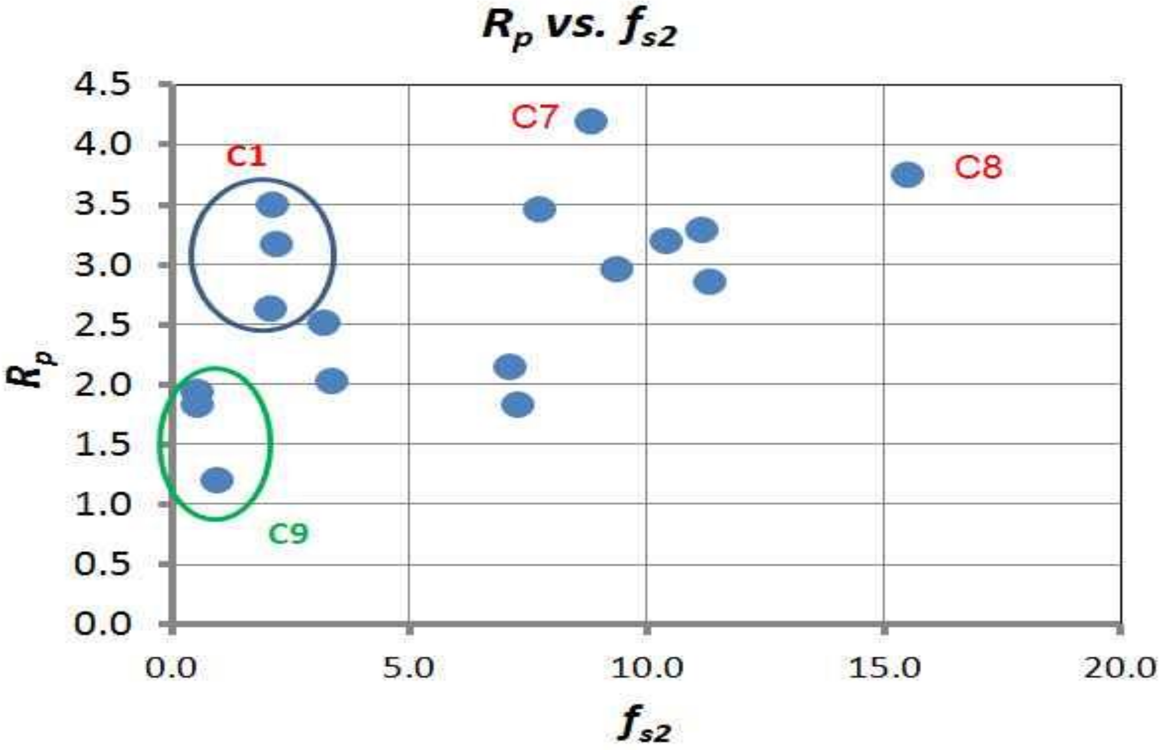

Statements of Blomshield

- If one increases burning rate with catalysts, propellant combustion response will tend to go down. (……every catalyst? not clear)
- Higher pressure exponents imply larger instability. Desirable to seek low *n* propellants.
- If one increases burning rate with fine AP, propellant combustion response will tend to go up.

- Very fine or very coarse AP is not good from a combustion instability point of view. These effects can be explained by the following -

  for very fine AP crystals burning in a fuel binder, chemical reaction processes are kinetically controlled and have a relatively high reaction order.

  for very large AP crystals, combustion is controlled by an AP mono-propellant flame which also has a high reaction order.

  in-between the extremes of particle size, combustion processes are believed to be controlled by more diffusional effects which are not as sensitive to pressure oscillations

Comment: Many of these statements could be correct, but experience suggests that following them without considering other basic features does not help.

From Blomshield and others – Response function

- AP pellets, at 34 atm, R_p = 2.0 to 1.5 ± 0.5 (decrease with frequency)
  AP pellets, at 70 atm, R_p = 1.5 to 2.4 ± 0.5, *n = 0.77*
  AP pellets, at 120 atm, R_p = 0.6 to 0.7 ± 0.5 (increase with frequency)

- RDX pellets, at 34 atm, R_p = 0.8 to 1.2 ± 0.3 *n = 0.82*
  RDX pellets, at 70 atm, R_p = 0.2 to 0.5 ± 0.1

- HMX pellets, 10 to 70 atm, R_p = 1.2 to 1.5 ± 0.3 *n = 0.85*

- AP (84%)-HTPB, at 15 atm, R_p = 0.6 to 0.9 ± 0.2 pressure index, *n= 0.45*
- AP (88%)-HTPB, at 34 atm, R_p = 0.4 to 0.7 ± 0.2 *n= 0.45*

Comment: The response function is expected to vary with pressure index. This is not always true as at increased pressures, the results do not show the appropriate trend.

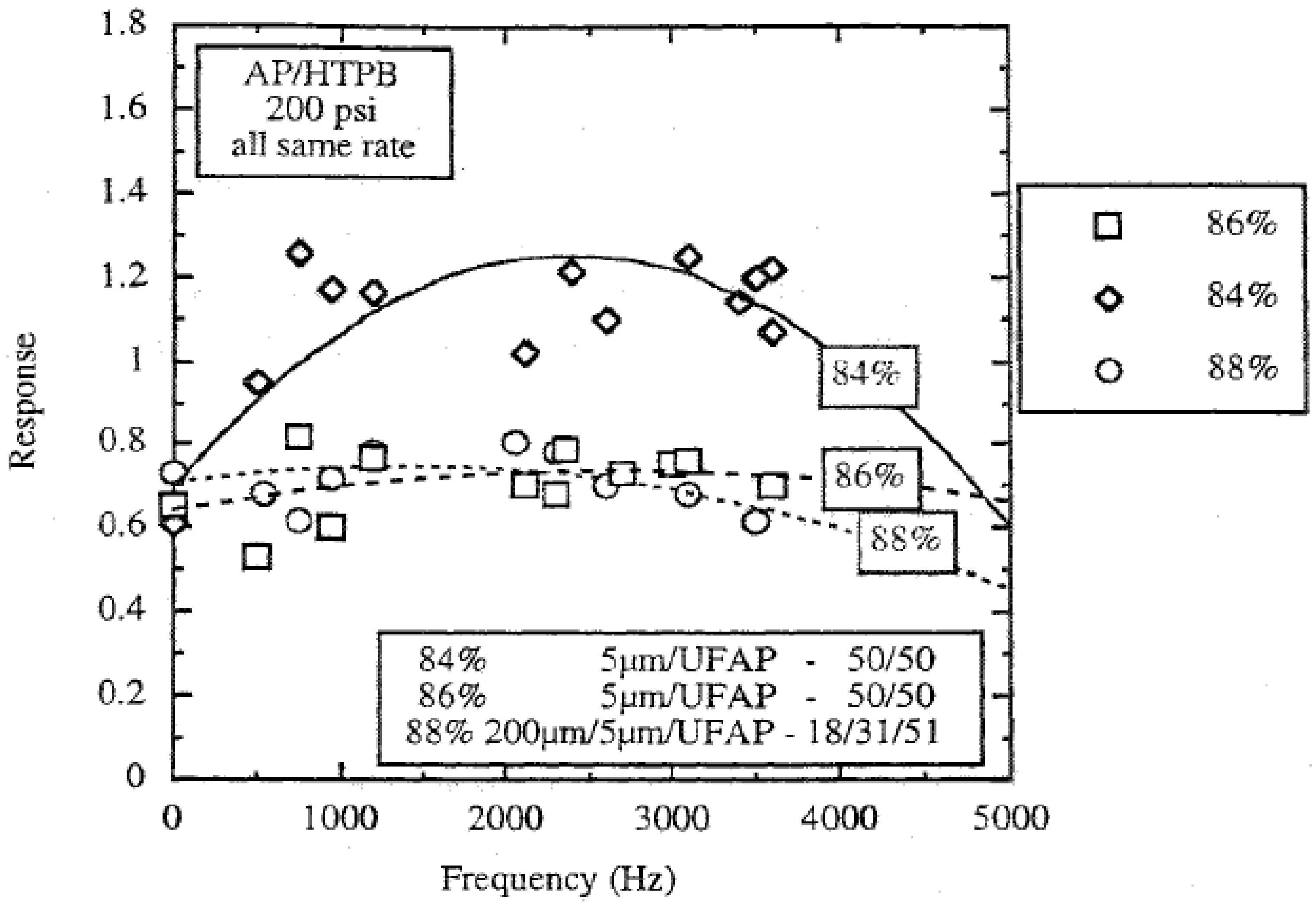

Figure 5. Influence of fine AP on the response for ~88% AP/HTPB propellant. (Crump's data Ref.9).

High energy AP-HTPB propellants have Rp ~ 0.6 to 1.2

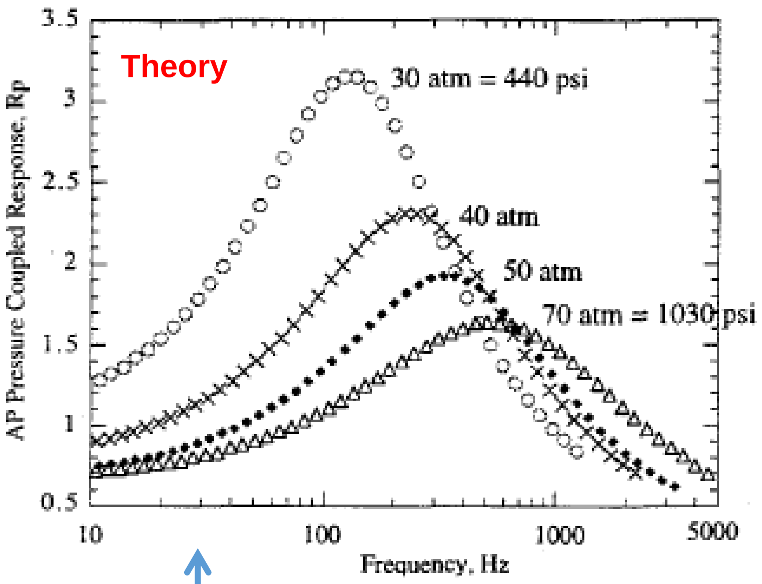

Beckstead’s predictions (AP) show that increased pressure implies reduced response.
In actual systems the behavior is contrary.

Many composite propellants (and double base propellants) have a pressure-coupled response evaluated by the T-burner have a response peak of 2 – 3 with an omega at around 7 (if you divide it by 2 π, this is about 1)

From Finlenson, Stalnaker and Blomshield, Ultra pure AP T-burner pressure coupled Response at 500, 1000 and 1800 psi AIAA 1998 – 3545, 34th AIAA Joint Prop conf.

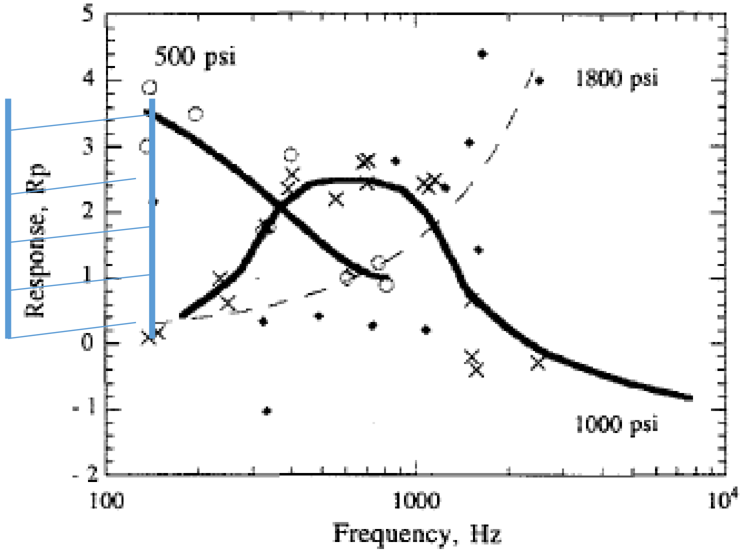

Figure 14. Pressure Coupled Response plot for UPAP pellets at 500, 1000, and 1800 psi.

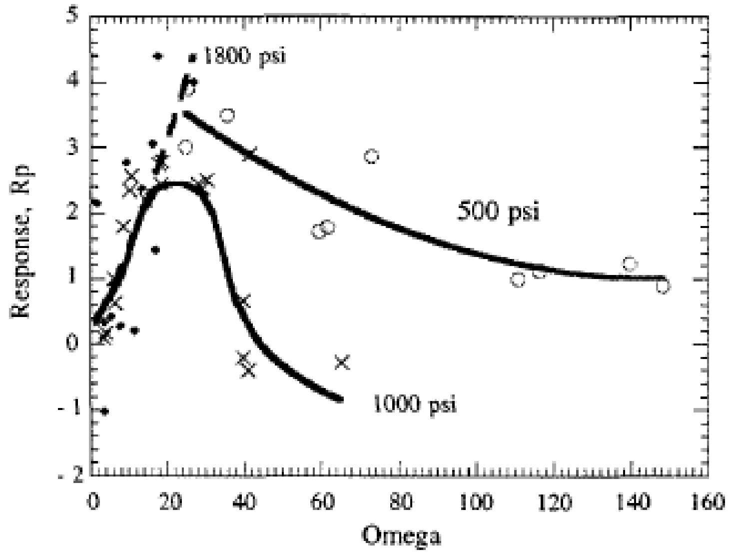

Omega = 2 pi (freq) α)/$\dot{r}^2$

Figure 15. Pressure Coupled Response plot for AP pellets at 500, 1000, and 1800 psi plotted vs. Omega.

From the thesis of Perry, Cal Tech, 1971

Propellant	A-13	T-17	540-A	A-35
Binder/Oxidizer	PBAN[1]/AP[2]	PS[3]/AP	PPG[4]/AP	PU[5]/AP
Specific Heats Ratio, γ	1.28	1.25	1.22	1.25
Density (gm/cm^3)	1.56	1.58	1.63	1.58
Burning Rate at 300 psig (cm/s)	0.48	0.78	0.50	0.46
Burning Rate Exponent at 300 psig	0.42	0.38	0.15	0.0
Flame Temperature at 300 psig (^{o}K)	2100	2050	2900	2160

……….The fact that the present T-burner investigations found 540 – A to be far from stable In this pressure range indicates again the lack of a thorough understanding of combustion instability in solid propellants……….

The situation is not very from this even now!

A subtle question ignored in the literature.

- The time scale of the fluctuations at 250 to 1000 Hz is 4 to 1 ms.
- At burn rates of 7 to 10 mm/s, the regression in 4 ms is 28 to 40 microns and in 1 ms, 7 to 10 microns. If we take 10 - 20 cycles as needed for response, the burn amount is 10 to 200 microns.
- These values are comparable to particle sizes in most propellants.
- This means that unless the scale of heterogeneity is accounted for, there is little chance of capturing the steady or unsteady combustion behavior.
- The model currently in wide use propagated by Culick has no aspects of heterogeneity in it. This is the reason for "backwardness" in understanding and combating instability in composite propellants.

$$R_p = \frac{nB + n_s(\lambda - 1)}{\lambda + \frac{A}{\lambda} - (1 + A) + B}$$

$$L = \frac{L_s}{c\overline{T}_s}$$

$$A = (1 - \frac{T_c}{\overline{T}_s})(\alpha_s + \frac{E_s}{R_o\overline{T}_s})$$

$$A = \frac{E_S(T_S - T_O)}{R_O T_S^{\,2}}$$

$$B = \frac{1}{\sigma_P(T_S - T_O)}$$

AN EXPERIMENTAL STUDY ON LOW-FREQUENCY COMBUSTION INSTABILITY OF COMPOSITE PROPELLANTS Masafumi Tanaka[1] and Kazunori Nakaji[1]

Links between steady and unsteady combustion

- Low pressure index, *n* is desirable from steady combustion view point. This does not mean ones needs to below the normal composite propellant burn rate index of 0.4 because the instability is not directly linked to *n in reality (Perry's thesis – 1971).*
- Liquid layer over the propellant surface may be the principal cause of the problems. If this is reactive, it is more serious (this is a new surmise not explicit in the literature).
- It is preferable to have as low a melt layer as possible. Perhaps, particle size distribution should avoid too much of coarse or fine particles. Very fine particles may bring down binder thickness but also lower the local air-fuel ratio encouraging melt layers.
- If ingredients are needed to be added to tailor the burn rate, it is useful to seek high melt temperature ingredients or those that encourage charring of the binder.

Some important features of steady combustion

AP and 1/7 propellant burn behavior

premixed flame structure with burn rate, ***r* (AP),** mm/s

$= 8.4\,(p_c/68)^{0.77}$ ($p_c > 20$ atm)

***r* (1 µm/7µm propellant)**

$= 32\,(p_c/68)^{0.75}$

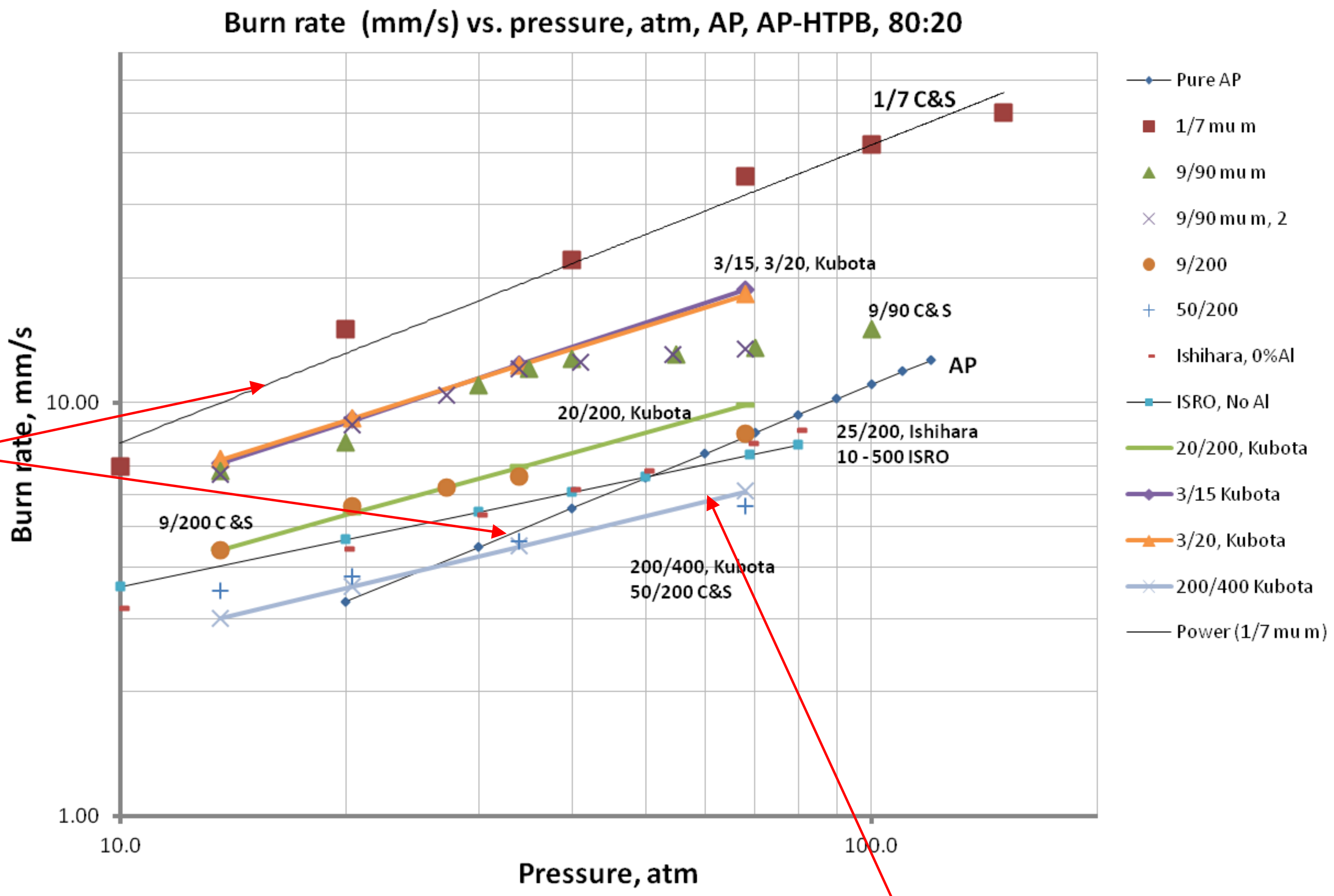

At lower ***p***, the energy from the diffusion flame enhances the burn rate significantly.
The burn behavior at higher ***p*** is controlled more by AP and hence, the burn rate approaches the burn rate of AP.
In this process, the value of pressure index comes down.

Notice that some burn rate curves intersect that AP curve and the burn rate is below that of AP.
This means that energy from the gas flame is being shielded by surface phenomena, presumably melt layers of fuel?

Modeling the heterogeneous aspects of composite propellant combustion

Heterogeneous Quasi-OneD model (HeQOD-M)

The HeQOD-M - features

- First to examine AP/HTPB composite propellants based on sequential burning approach accounting for,
  - Heterogeneity and the associated local O/F and flame temperature variations.
  - Detailed particle size distribution.
  - Premixing of fuel and oxidizer.
  - Extinction of very fuel rich small AP particles - a new phenomenon not captured by earlier models.

The process

Since the line average intersection of spherical particles in a random packing is proportional to the corresponding volume fraction (Iyer et al. (2015))

$$l_{avg} \propto V_{fraction}$$

- When coated with binder matrix of thickness tb, line average intersection will become:

- The burn rate of the propellant can be calculated as:

Burn rate = $\dfrac{\text{Length of entire line}}{\text{Total time taken by line to burn}}$

$$l_j = \frac{V_j(1+2t_b/d_j)}{\Sigma_j V_j(1+2t_b/d_j)}$$

$$\frac{1}{\dot{r}} = \Sigma[\frac{l_j(d_j)}{\dot{r}_j(d_j)}]$$

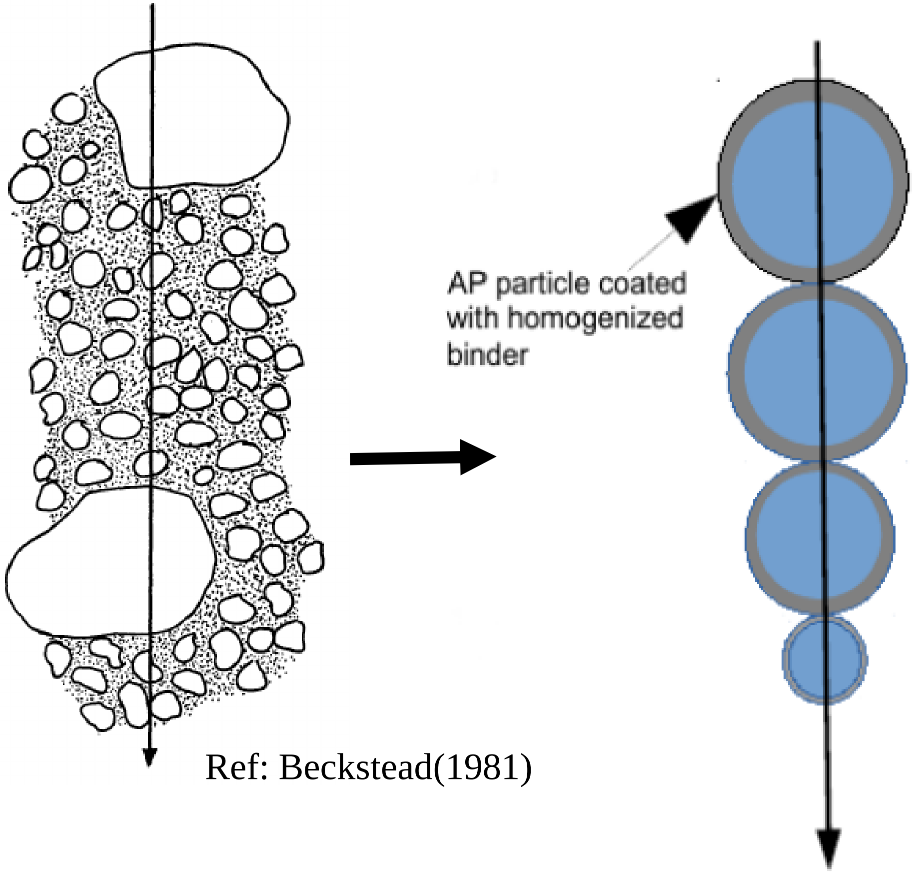

Ref: Beckstead(1981)

The rest of the model description is to determine the burn of each AP particle surrounded by binder.

Modeling Features (AP & propellant)

Regressing surface is planar; Condensed phase is homogeneous and 1-D as far as conduction in solid is concerned; The gas phase flame is thin and gas phase temperature profile is one-dimensional.

The diffusion flame process is set out to obtain the average heat transfer to the AP particle affected by particle size, binder aspects and pressure.

Model for AP combustion

$$\xi = \rho_p \dot{r} c_p x / k_g$$

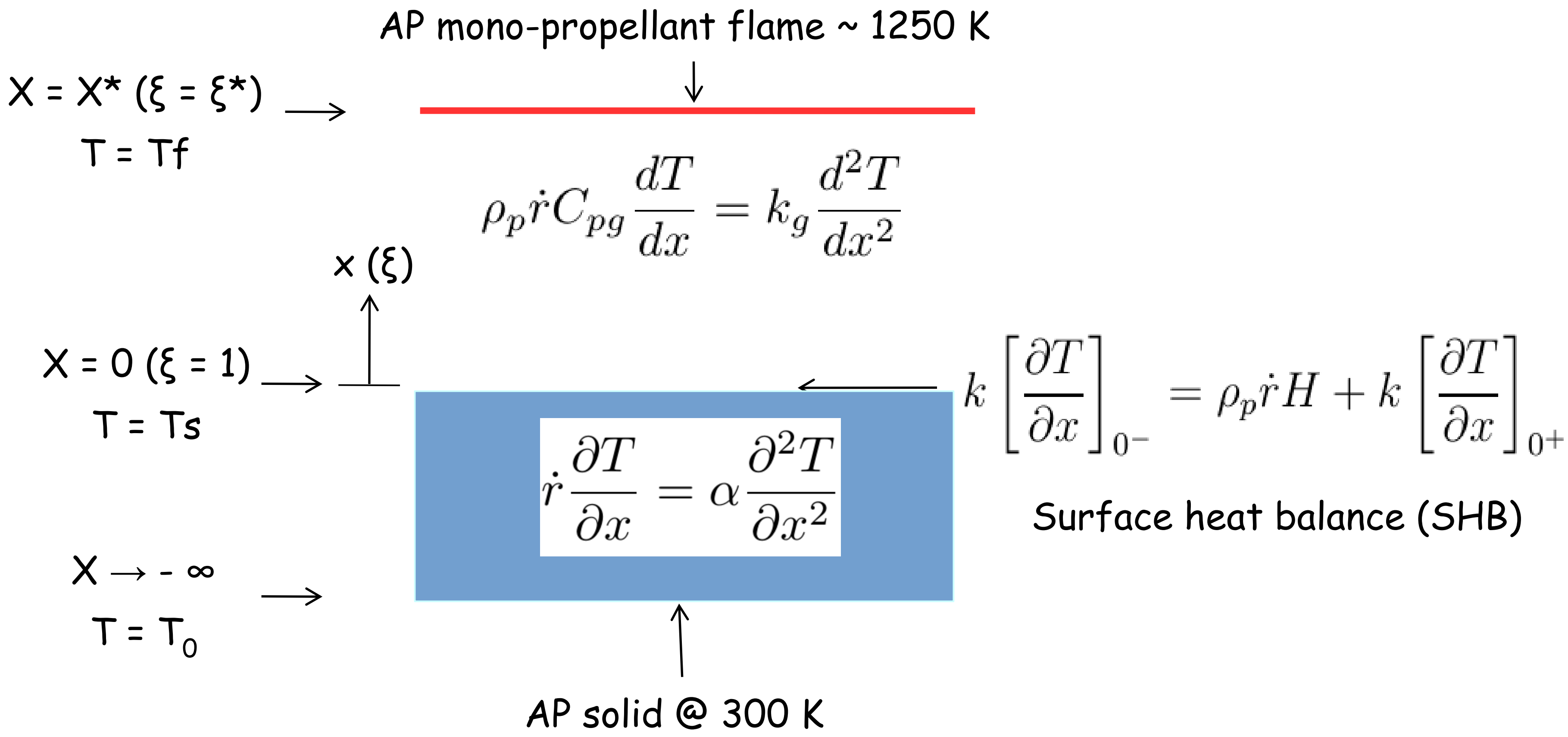

Contd ...

Surface heat balance $\rho_p \dot{r} c_p (T_s - T_0) = \rho_p \dot{r} H + \rho_p \dot{r} c_p (T_f - T_s)/(\xi^* - 1)$

$x^* = \frac{k}{\rho_p \dot{r} c_p} ln[1 + \frac{c_p(T_f - T_s)}{c_p(T_s - T_0) - H_{AP}}]$ - On substituting for $\xi^* = \rho_p \dot{r} c_p x^*/k$

Mass balance (for gas phase chemical reaction) $\rho_p \dot{r} = K_{r,AP} p^{n_r} x^*$

$$\boxed{\rho_p \dot{r} = \sqrt{\frac{k_g}{c_{pg}} ln(1 + B_{AP}) p^{n_r} K_{r,AP}}}$$

$$\boxed{\dot{r} = A_s exp(-E_s/RT_s)}$$ $\longrightarrow$ Pyrolysis law

Simultaneous solution of mass balance and pyrolysis law equations will give the burn rate of AP, if other parameters are known.

AP thermo-physical, transport and kinetic parameters

Parameter (units)	Value	Reference
E_s/R (K)	6500	Ramakrishna (2000)
T_s @ 20 atm (K) – AP melting temperature	850-870	Ramakrishna (2000)
A_s (mm/s) – calculated using E_s/R, T_s and r (3.3 mm/s) @ 20 atm	5798	-
K_g (W/m-K)	0.08	-
C_p (J/kg-K)	1150	Hanson & Parr (1999)
H/C_p (K)	400-500	Langelle et al(2002)
K_r (gas phase reaction rate)	1000	Estimated from conditions at 20 atm
n_r (reaction order)	2	

Parameter range around the suggested values explain the observed burn rate, index and temperature sensitivity of AP.

Burn rate model for AP particle surrounded by binder matrix

Propellant	200μ	50μ	20μ	6μ	2μ	0.7μ
SD-III-4	36.15		27.7			36.15
SD-III-9	36.15		27.7		36.15	
SD-III-14	36.15		27.7	36.15		
SD-III-19	36.15		27.7+36.15			
SD-III-16	36.15	36.15	27.7			

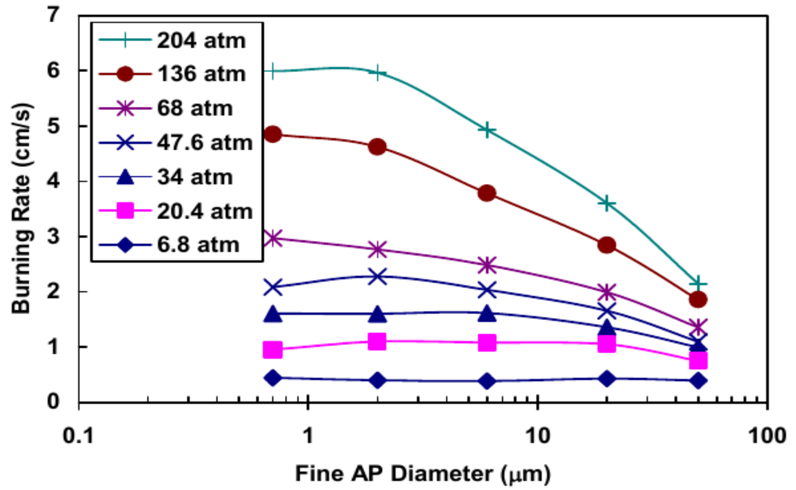

Particle size effect on AP/HTPB propellant

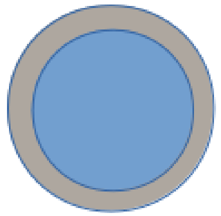

AP particle coated with binder

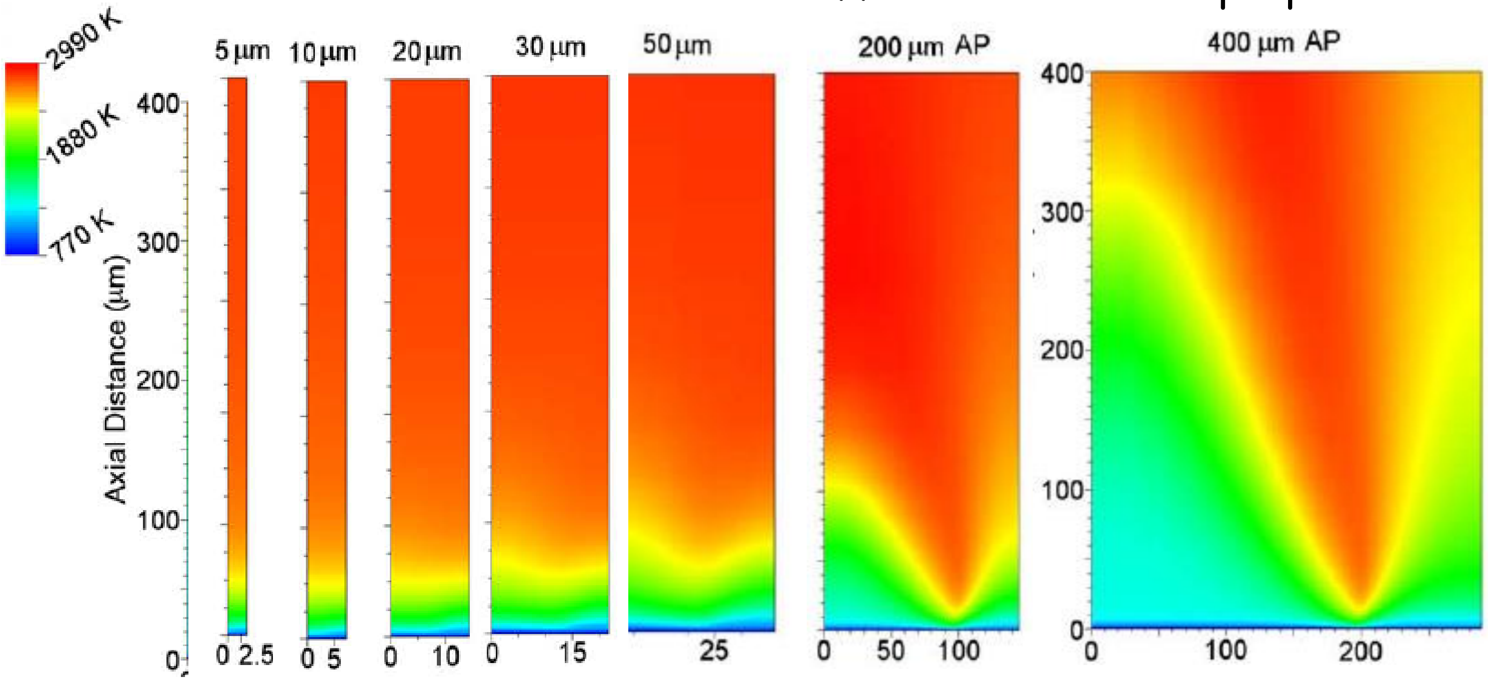

AP size increases

Ref:Gross-Beckstead(2009)

From: Gross and Beckstead (2000)

The effective flame temperature

$$\frac{T_{eff} - T_{f,AP}}{T_{f,ad} - T_{f,AP}} = \frac{1 - e^{-Z}}{Z}$$

$$z = \left(\frac{d_{AP}}{d_0}\right)(1 - \phi)$$

where $d_0 = (d_{ref} + 2t_b)\left(\frac{20}{p}\right)^m \left(\frac{K_{e,premixed}}{K_{r,AP}}\right)^{0.5}$

$d_{ref} \sim \sqrt{Dt_r}$

T_{eff}	effective flame temperature (K)
$T_{f,ad} = f(O/F)$	adiabatic flame temperature (K)
$T_{f,AP}$	adiabatic flame temperature of AP (K)
d_{AP}	AP particle diameter (μm)
$d_0 \sim \sqrt{Dt_r}$	reference diffusion distance (90 μm)
D	diffusion coefficient
t_r	reaction time
ϕ	binder equivalence ratio
t_b	binder thickness (μm)
$m = f(\phi)$	pressure coefficient of reaction rate

$$d_{AP} \to 0 \Rightarrow f(Z) \to 1 \Rightarrow T_{eff} = T_{f,ad}$$

$$d_{AP} \to \infty \Rightarrow f(Z) \to 0 \Rightarrow T_{eff} = T_{f,AP}$$

Effective reaction rate

The effective reaction rate depends on the effective flame temperature – Arrhenius type relation

The Arrhenius coefficients can be determined from the gas phase reaction rate for AP mono-propellant flame and fine AP/HTPB premixed flame.

Limits	$T_{f,ad}$ (K)	K_r (s/m^2atm)
AP mono-propellant flame	1250	1000
AP/HTPB premixed flame (86% AP)	2850	30000

$$\downarrow$$

$$K_{r,eff} = 4.3e5e^{-7573/T_{eff}}$$

$$\rho_p \dot{r}\left[c_p(T_s - T_0)\right] = \rho_p \dot{r} H_{eff} + \frac{\rho_p \dot{r} c_p (T_{eff} - T_s)}{e^{\xi^*} - 1} g_f$$

$$\xi^* = ln(1 + B_{eff})$$

$$B_{eff} = \left[\frac{T_{eff} - T_s}{T_s - T_0 - H_{eff}/c_p}\right] g_f$$

$$g_f = \begin{cases} \frac{d_{AP}^2}{(d_{AP}+2t_b)^2} & \text{if } \phi < 0.7 \\ 1 & \text{otherwise} \end{cases}$$

Binder thickness, O/F and adiabatic flame temperature

Binder thickness is calculated by assuming that HTPB mixed with fine AP (<6 μm) is coated with uniform thickness (tb) on the surface of AP particles of size (> 6 μm)

$$\frac{f_{HTPB}}{\rho_{HTPB}} + \frac{f_{AP<6\mu m}}{\rho_{AP}} = \Sigma_i \frac{f_{AP,i}}{\rho_{AP}} \left[(1 + 2t_b/d_i)^3 - 1\right]$$

f_{HTPB}	mass fraction of HTPB
$f_{AP<6}$	mass fraction of AP with size $< 6\ \mu m$
$f_{AP,i}$	mass fraction of AP with size d_i (with $d_i > 6\ \mu m$)
ρ_{AP}	density of AP ($1950\ kg/m^3$)
ρ_{HTPB}	density of HTPB ($930\ kg/m^3$)

$$O/F = \frac{\rho_{AP} + \rho_b \left[(1 + 2t_b/d_i)^3 - 1\right] SL_b}{(1 - SL_b)\rho_b \left[(1 + 2t_b/d_i)^3 - 1\right]}$$

$T_{f,ad}$ is obtained from O/F using equilibrium calculation

$$\rho_b = \frac{f_{HTPB} + f_{AP<6\mu m}}{f_{HTPB}/\rho_{HTPB} + f_{AP}/\rho_{AP}} \qquad SL_b = \frac{f_{AP<6\mu m}}{f_{HTPB} + f_{AP<6\mu m}}$$

The burn rate equation

The burn rate of AP particle of size d_i coated with binder of thickness t_b is calculated by solving this equation simultaneously with the AP pyrolysis law

$$\rho_p \dot{r} = \sqrt{\frac{k_g}{c_{pg}} ln(1 + B_{eff}) p^{n_r} K_{r,eff}}$$ **with** $$\dot{r} = 5.8 exp(-6500/T_s) \ (mm/s)$$

Following this the model was used to predict the burn rate for the following cases –

1) Sandwich propellant modeled in Gross & Beckstead (2010)
2) 87.4% AP loaded propellants reported in Miller (1982)
3) 2 propellants made by PEL produced on our request
4) Propellants reported by Fredrick

Model validation with results of Gross and Beckstead (2010)

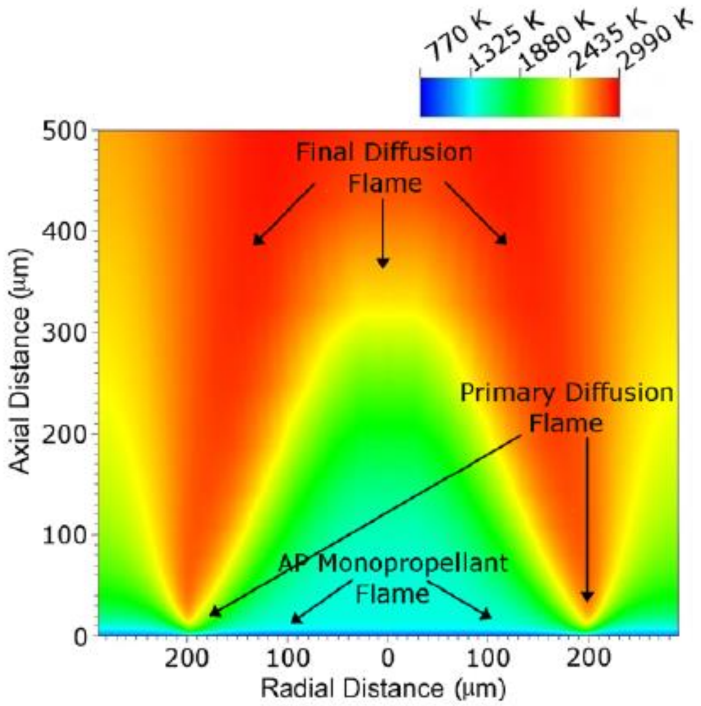

Fig. 1. Flame structure above a 400 μm AP particle surrounded by 89 μm of binder at 20 atm.

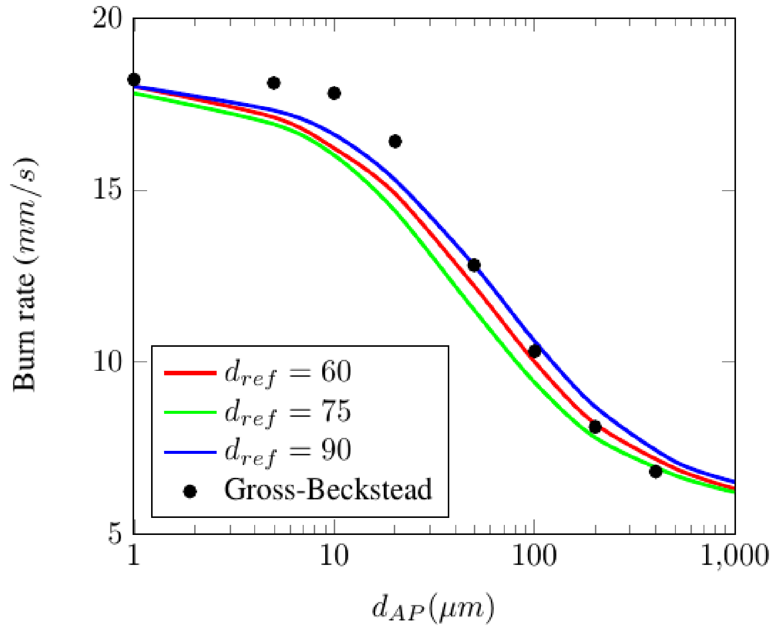

Comparison of current model predictions with results from with Gross-Beckstead (2010)

These results were obtained by performing CFD calculations with detailed chemistry for decomposition of AP, reaction of AP decomposition products with HTPB etc. Burn rate results were obtained by varying the particle size from as small as 5 to 500 μm. Comparison of these results clearly show that the same results can be obtained with much greater simplicity – excel sheet/matlab like calculations.

Critical extinction size limit – a new feature of the model

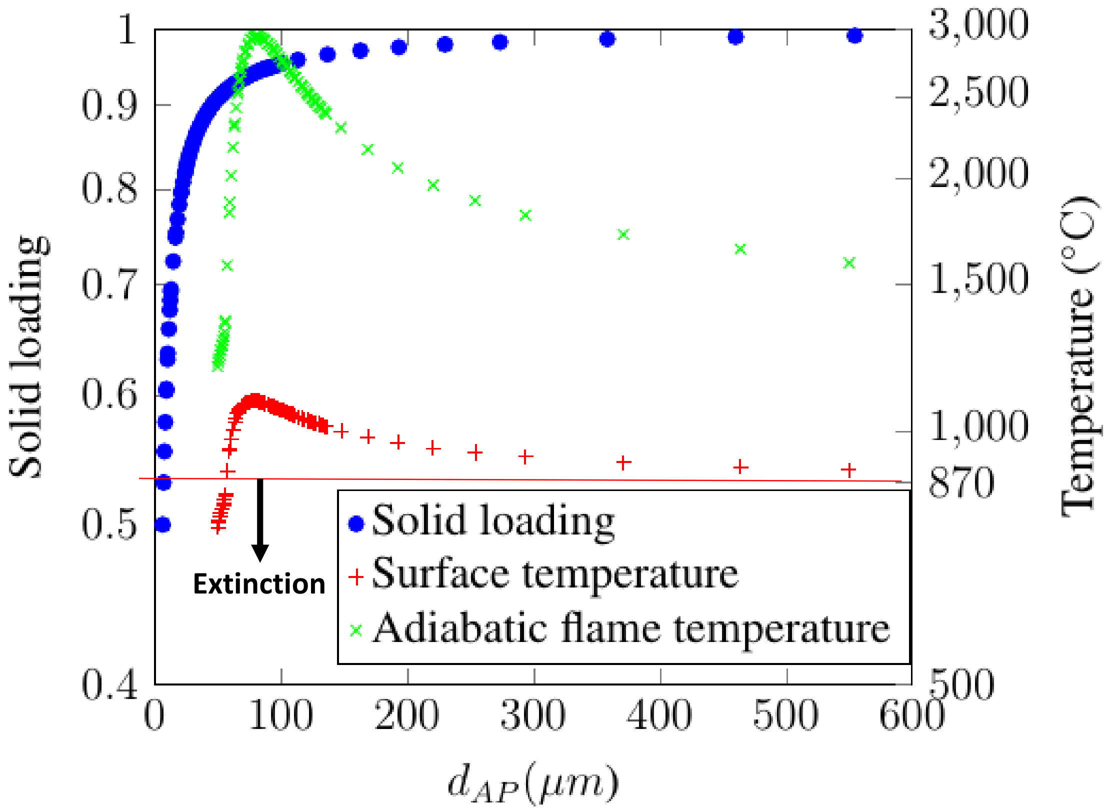

- AP particles of size <6μm is homogenized with the binder – premixed flame limit
- In addition to this if the local O/F of a particular particle size is very less compared to the stoichiometric value (7.33) extinction will occur – rich flammability limit

$$O/F = \frac{\rho_{AP} + \rho_b\left[(1+2t_b/d_i)^3 - 1\right] SL_b}{(1-SL_b)\rho_b\left[(1+2t_b/d_i)^3 - 1\right]}$$

Also under very rich conditions the heat flux received by the AP surface may not be sufficient to raise the surface temperature beyond 870 K (the melting temperature of AP). This will also cause extinction.

Particle sizes less than the critical extinction size, determined using an iterative procedure, is added to the binder and then distributed with uniform thickness over all other particles undergoing deflagration.

Experimental data from Miller (1982)

Table III. Strand Burn Rate Results

Propellant Designation	Average Burn Rate (cm/sec) at Pressure (MPa) 0.69	2.07	3.45	4.83	6.89	13.8	20.7
SD III-2	.523	.965	1.53	-	2.95	5.61	7.44
SD III-3	.579	1.32	2.34	2.59	3.68	5.82	7.16
SD III-4	.442	.953	1.61	2.09	2.97	4.85	5.99
SD III-5	.340	.683	1.20	1.64	2.21	4.32	6.17
SD III-6	.551	1.40	1.87	2.43	2.95	4.42	5.77
SD III-8	-	-	1.73	-	2.79	4.50	-
SD III-9	.401	1.10	1.60	2.28	2.77	4.62	5.97
SD III-10	.330	.808	1.27	1.90	2.29	4.06	5.64
SD III-12	.450	1.19	1.72	2.16	2.62	4.04	5.36
SD III-14	.386	1.08	1.62	2.04	2.48	3.79	4.93
SD III-15	.284	.823	1.14	1.51	1.79	2.97	4.09
SD III-16	-	-	1.03	-	1.43	1.93	-
SD III-17	.472	1.13	1.53	1.81	2.12	2.95	3.73
SD III-18	.483	1.02	1.32	1.54	1.82	2.43	3.07
SD III-19	.427	1.05	1.36	1.66	1.99	2.85	3.61
SD III-20	.300	.759	.935	1.12	1.37	2.17	2.85
SD III-21	.287	.498	.610	.716	.838	1.11	1.41
SD III-22	.389	.742	.953	1.09	1.33	1.80	2.12
SD III-23	.381	.663	.843	.973	1.19	1.60	1.87
SD III-24	.394	.752	.998	1.10	1.36	1.86	2.15
SD III-25	.302	.612	.772	.912	1.13	1.66	1.94
SD III-26	-	-	1.20	-	1.63	2.12	-
SD III-27	-	-	.678	-	.975	1.66	-
SD III-28	-	-	.701	-	.978	1.58	-
SD III-29	-	-	.704	-	.942	1.22	-
SD III-30	-	-	1.21	-	1.71	2.54	-
SD III-31	-	-	.653	-	.930	1.58	-
SD III-32	-	-	.947	-	1.58	2.44	-
SD III-33	-	-	-	-	1.47	-	-

Table I. Summary of Propellant Composite Data

Propellant Designation	Relative Wt% of Nominal AP Size Fraction								Average Sizes			
	400µ	200µ	90µ	50µ	20µ	6µ	2µ	0.7µ	$d_{4,3}$	$d_{3,2}$	$d_{2,1}$	$d_{1,0}$
SD III-2	-	-	36.15	-	15.66	-	-	48.19	33.7	.96	.22	.14
SD III-3	-	-	-	-	63.85	-	-	36.15	17.9	1.2	.22	.14
SD III-4	-	36.15	-	-	27.70	-	-	36.15	86.8	1.3	.22	.14
SD III-5	48.19	-	-	-	15.66	-	-	36.15	221	1.3	.22	.14
SD III-6	-	-	-	36.15	15.66	36.15	12.04	-	23.7	5.8	2.3	1.6
SD III-8	-	-	-	36.15	27.70	-	36.15	-	24.9	4.4	1.8	1.4
SD III-9	-	36.15	-	-	27.70	-	36.15	-	86.7	4.5	1.7	1.4
SD III-10	48.19	-	-	-	15.66	-	36.15	-	221	4.7	1.7	1.4
SD III-12	-	-	36.15	-	15.66	48.19	-	-	35.8	7.8	3.1	2.0
SD III-14	-	36.15	-	-	27.70	36.15	-	-	88.3	9.7	3.2	2.0
SD III-15	48.19	-	-	-	15.66	36.15	-	-	222	10.4	3.0	2.0
SD III-16	-	36.15	-	36.15	27.70	-	-	-	103	37.8	17.3	10.0
SD III-17	-	-	36.15	-	63.85	-	-	-	45.1	24.8	13.9	8.9
SD III-18	-	-	48.19	-	51.81	-	-	-	51.6	28.1	14.8	9.1
SD III-19	-	36.15	-	-	63.85	-	-	-	95.3	27.1	13.1	8.7
SD III-20	48.19	-	-	-	51.81	-	-	-	230	34.1	12.9	8.7
SD III-21	36.15	36.15	-	12.04	15.66	-	-	-	251	68.6	18.1	9.6
SD III-22	36.15	-	-	48.19	15.66	-	-	-	189	46.1	20.0	11.3
SD III-23	-	48.19	-	36.15	15.66	-	-	-	127	48.6	20.4	11.0
SD III-24	-	36.15	-	48.19	15.66	-	-	-	106	43.5	20.8	11.5
SD III-25	48.19	-	-	36.15	15.66	-	-	-	238	53.0	19.1	10.8
SD III-26	-	-	53.20	-	46.80	-	-	-	54	29.7	15.3	9.2
SD III-27	59.00	-	-	-	25.00	-	16.00	-	266	9.5	1.8	1.4
SD III-28	54.50	-	-	13.00	32.50	-	-	-	254	44.7	14.6	9.1
SD III-29	50.00	-	36.00	-	-	14.00	-	-	242	24.9	3.3	2.0
SD III-30	-	37.88	-	-	62.12	-	-	-	99	27.8	13.2	8.7
SD III-31	59.00	-	-	-	8.95	-	32.05	-	268	6.4	2.0	1.7
SD III-32	48.19	-	-	-	33.49	-	18.32	-	216	8.1	2.1	1.6
SD III-33	48.19	-	-	-	42.65	-	9.16	-	226	13.2	2.3	1.6

Features -

- High solid loading – 87.4%
- Covers a particle size range from 0.7 – 400 µm
- Includes bi-, tri- and multi-modal distributions
- A highly referenced work

On prediction quality for different propellants – particle size distributions

Note: Chemical kinetic parameters fixed. No free parameters

Total number of propellant predictions made - 44

Propellant	Quality	No.	Possible reason
Miller (1982)	Excellent	16	Physics embedded in the model
	Not too good	6	Excessive small sizes – only model propellants
	Poor	7	Excessive small sizes – only model propellants
Ramakrishna, IITM	Excellent	1	Physics embedded
PEL, Hyderabad	Excellent	1	Physics embedded
Frederick (1988)	Excellent	5	Physics embedded
	Poor	8	Excessive small sizes – only model propellants

A common feature of all propellants showing poor predictions is that they contain significant amounts of fine AP (<20 μm). Finer particles have the tendency to agglomerate and form larger particles.

Propellants with Excellent Predictions - examples

Miller (1982)

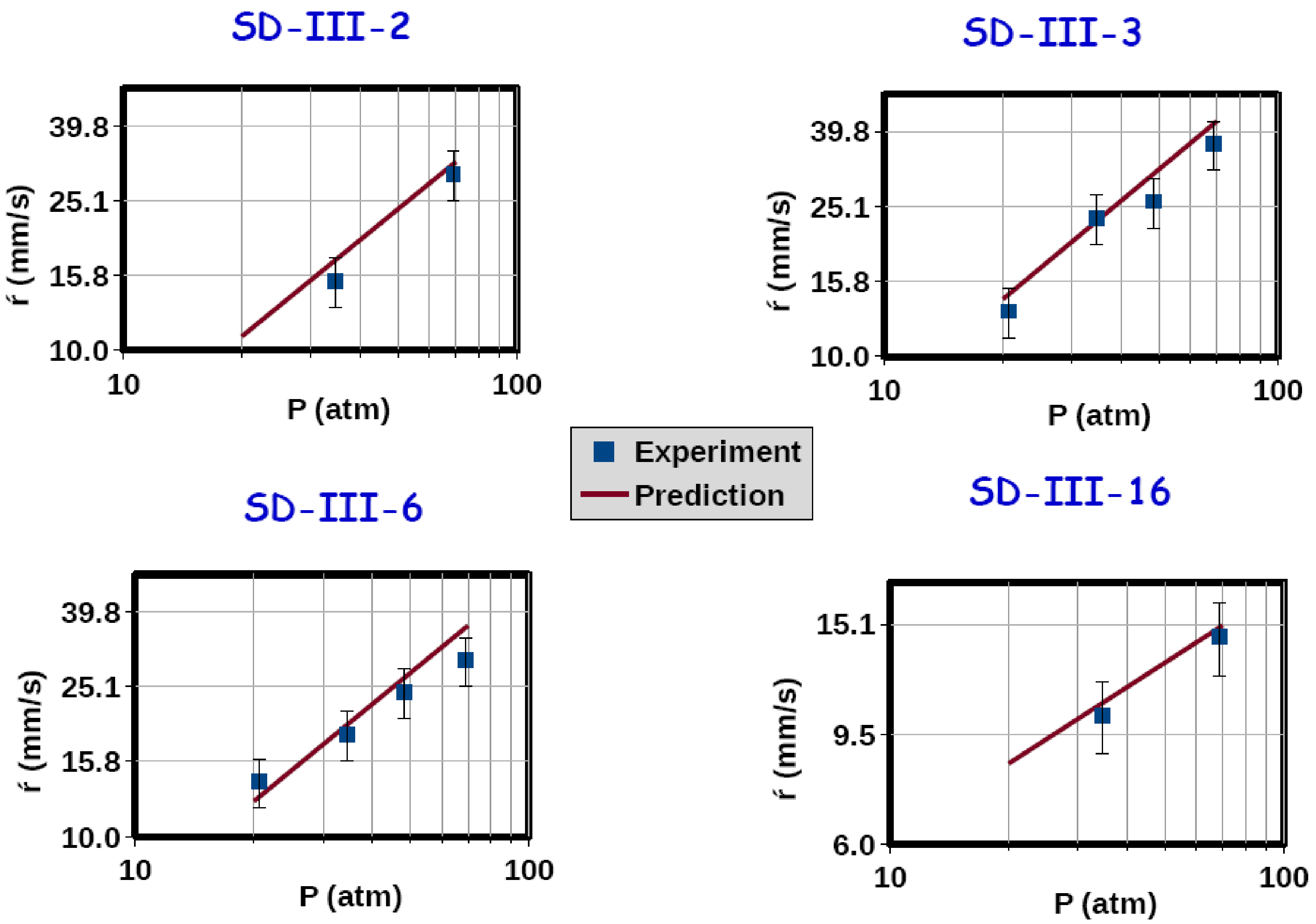

Fredrick (1988)

P

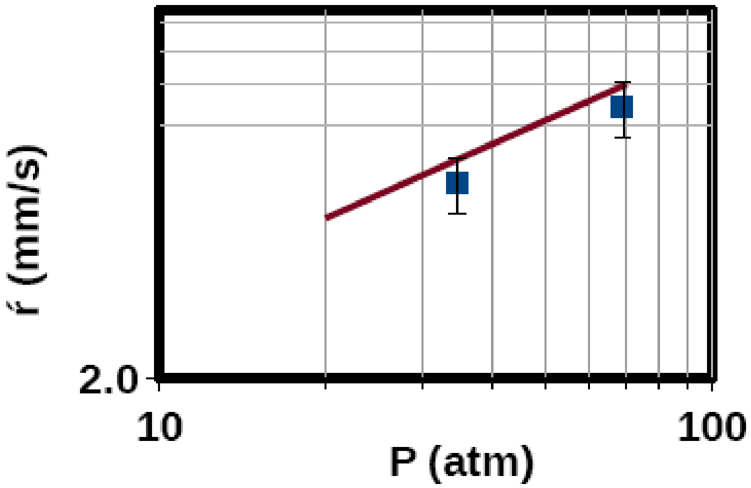

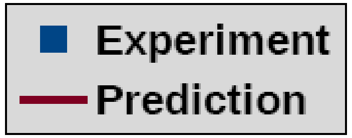

R&D-006

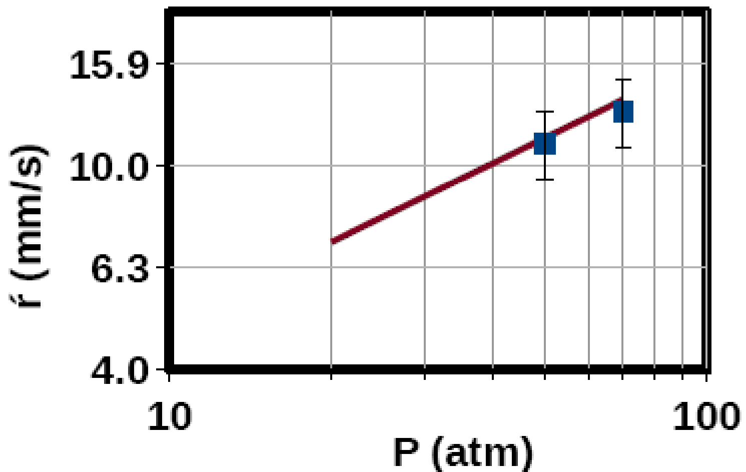

Kumar and Ramakrishna (2013)

Mix 1

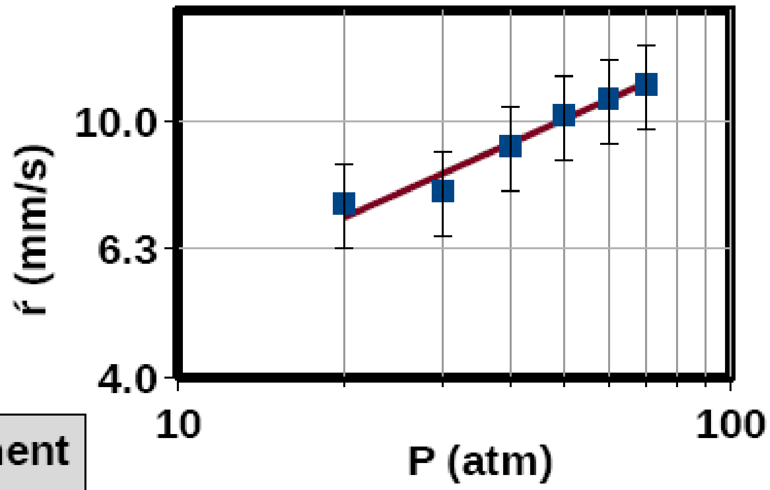

Not too good predictions - within 20 %

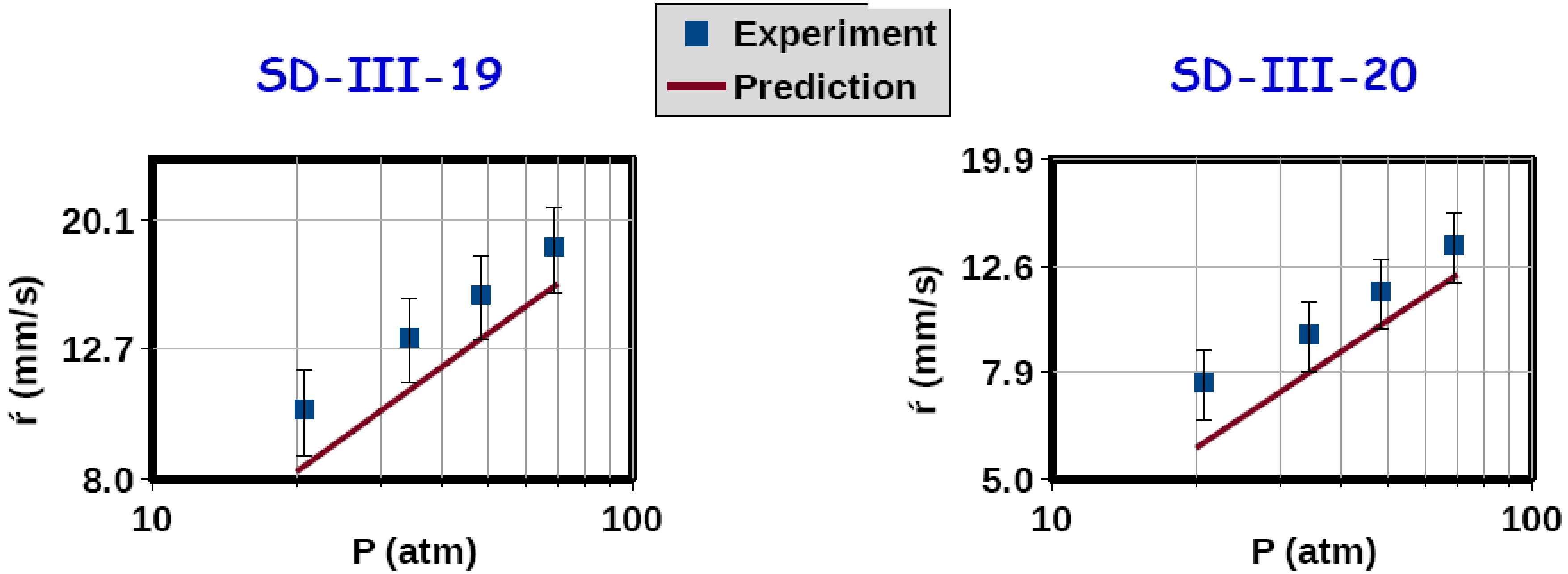

Poor predictions

Miller (1982)

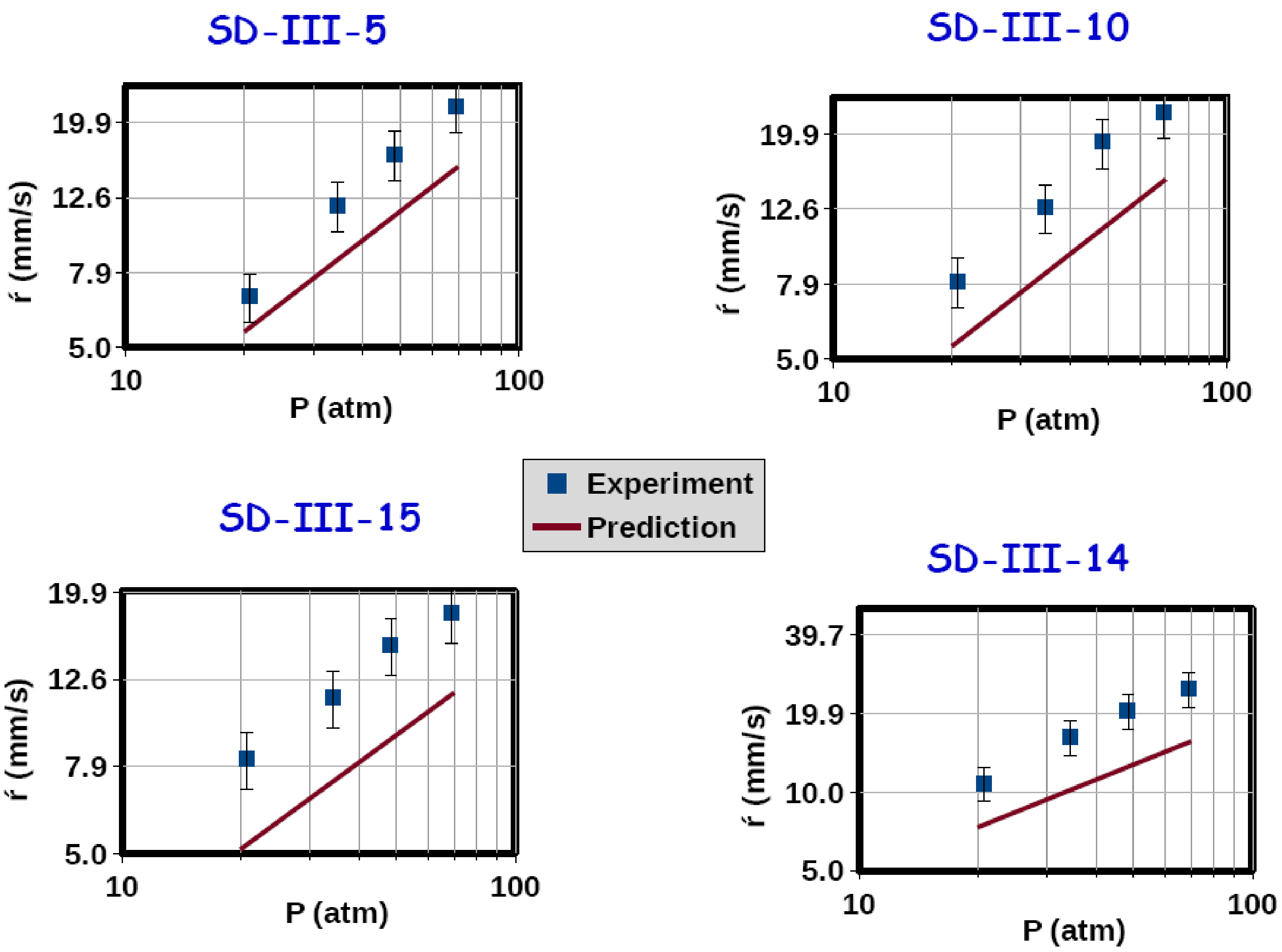

All these propellants have >35 % fine AP (6 microns, 2 microns and 0.7 microns)

Difficult to eliminate agglomeration unless the particles are suitably coated for the purpose. No such indications are available in the paper.

What further benefits from this model?

- We should recall that CFD as a tool has been used to aid design in the last ten years as it has become a well trusted tool.
- Trust arose out of a large number of good predictions, and when predictions were not so good, determine from studies corrections to the parameters (turbulence largely), etc.

- Similarly, it is suggested that the tool described here can be used for designing propellants – simple ones described here and more to come through with work already completed on Aluminum, RDX and some additives like $SrCO_3$.
- More calibration work on premixed high energy propellants with additives needs to be done.
- An example of what change in particle size distribution can do is shown……

Effect of coarse to fine ratio with different ultra fine fraction for TCL AP

Total Solid loading = 83%

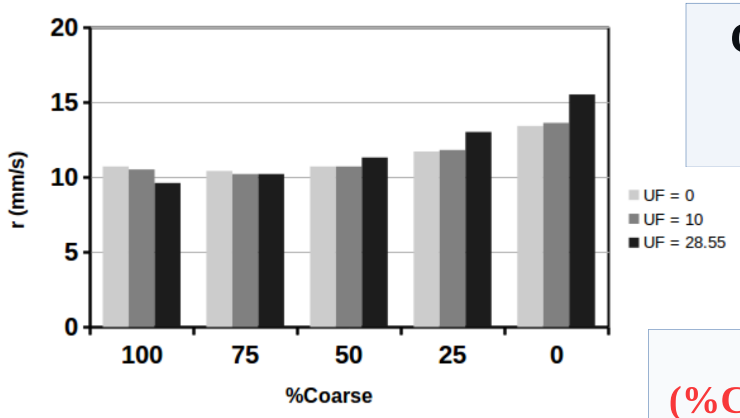

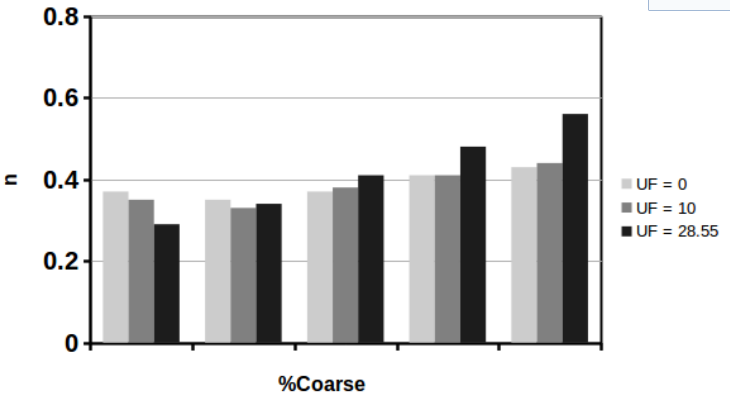

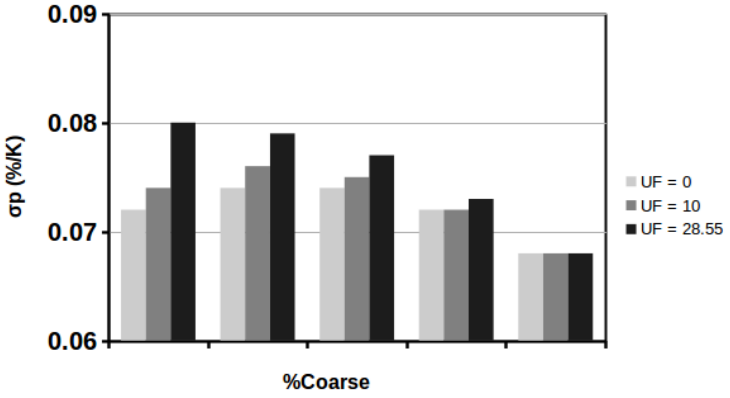

Coarse – 350 μm
Fine – 60 μm
UF – 9 μm

%Fine = SL – (%Coarse + %Ultrafine)

● Experiment

Total Solid loading = 86%

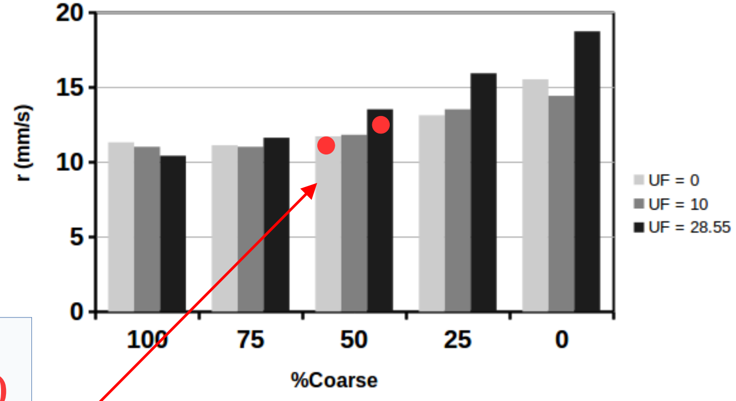

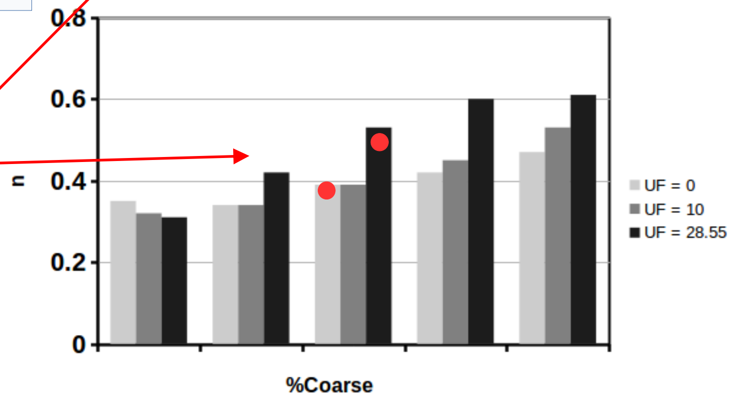

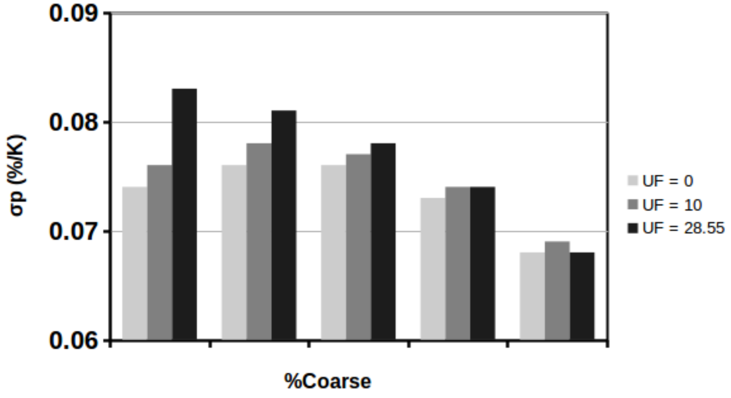

Studies on the effect of AP, HMX, RDX and $SrCO_3$

Source	Type	Number	Features
Miller (1982)	AP/HTPB	29	High solid loading - 87.4% Bi, tri and quad modal d_{AP} - 0.7 - 400 μm
Kumar & Ramakrishna (2014)	AP/HTPB	1	High solid loading - 86%
PEL	AP/HTPB	2	High solid loading - 85.65%
PEL	AP/HTPB/RDX	2	10% RDX in place of AP in the other two PEL propellants
PEL	AP/HTPB/$SrCO_3$	2	AP from two different sources used
Blomshield & Osborn (1990)	AP/HTPB/HMX	10	10-15% HMX substituted in place of AP in SD-III-10 and SD-III-25 of Miller (1982)

Table 5: Composition of PEL propellants

Prop. ID	AP (%)				RDX (%)	$SrCO_3$ (%)	Binder (%)
	325 μm	200 μm	60 μm	9 μm			
R-D-006	-	2[illegible]55	28.55	28.55	-	-	14.35
R-D-007	-	4[illegible]11	38.54	-	-	-	14.35
R-D-010		2[illegible]55	28.55	18.55	10	-	14.35
R-D-011		4[illegible]11	28.54	-	10	-	14.35
C9P5	54.53	27.27	-	-	-	2.5	15.7
C9P6	56.46	23.52	-	-	-	2.5	17.5

What is clear from a study of these propellants is that low burn rate index propellants can be dealt with within this frame work only by invoking the presence of liquid layer.

Produced by PEL at the request of the investigators to partly simulate Miller's data

What is therefore a scheme to deal with these aspects?

- Physics based steady combustion modeling of composite propellants has resulted in excellent predictions for known cases with no free parameter juggling

- Calibrated and trustworthy; additional comparison with experiments for more complex additives needs some special propellants to be made for calibration like fine AP-HTPB propellants with them.

- Response function calculation; comparison with experiments and full motor calculation to explain linear instability, DC shift and related behavior are future actions.

Thanks for your attention